Check for updates

Accepted Article

Productivity and dissolved oxygen controls on the Southern Ocean deep-sea benthos during the Antarctic Cold Reversal

Joseph A. Stewart [1*], Tao Li [1,2], Peter T. Spooner [1,3], Andrea Burke [4], Tianyu Chen [1,2], Jenny Roberts [5], James W. B. Rae [4], Victoria Peck [6], Sev Kender [7,8], Qian Liu [1], Laura F. Robinson [1]

[1] School of Earth Sci. Univ. of Bristol, Queens Road, Bristol, BS8 1RJ, UK
[2] School of Earth Sciences and Engineering, Nanjing University, 210023 Nanjing, China
[3] Department of Earth Science, University College London, London, UK
[4] School of Earth & Environmental Sci., Univ. of St Andrews, Irvine Building, KY16 9AL
[5] Thermo Fisher Scientific, Hanna-Kunath-Straße 11, 28199 Bremen, Germany
[6] British Antarctic Survey, High Cross, Madingley Road Cambridge, CB3 0ET, United Kingdom
[7] Camborne School of Mines, University of Exeter, Penryn Campus, Penryn, Cornwall, TR10 9FE, UK
[8] British Geological Survey, Environmental Sciences Centre, Keyworth, Nottingham, NG12 5GG, UK

*correspondence joseph.stewart@bristol.ac.uk

Key Points:

- Shallow Subantarctic sites show Antarctic Cold Reversal peaks in thick-walled benthic foraminifera and cold-water coral abundance.
- Corals were largely absent at deeper and more southerly sites during this interval.
- Northward displacement of productivity and low oxygen bottom waters were key to these changes in benthic ecology at 14 ka.

This article has been accepted for publication and undergone full peer review but has not been through the copyediting, typesetting, pagination and proofreading process, which may lead to differences between this version and the Version of Record. Please cite this article as doi: 10.1029/2021PA004288.

This article is protected by copyright. All rights reserved.

Accepted Article

Abstract

The Antarctic Cold Reversal (ACR; 14.7 to 13 thousand years ago; ka) phase of the last deglaciation saw a pause in the rise of atmospheric CO_2 and Antarctic temperature, that contrasted with warming in the North. A re-expansion of sea ice and a northward shift in the position of the westerly winds in the Southern Ocean are well-documented, but the response of deep-sea biota and the primary drivers of habitat viability remain unclear. Here we present a new perspective on ecological changes in the deglacial Southern Ocean, including multi-faunal benthic assemblage (foraminifera and cold-water corals) and coral geochemical data (Ba/Ca and $\delta^{11}B$) from the Drake Passage. Our records show that, during the ACR, peak abundances of thick-walled benthic foraminifera *Uvigerina bifurcata* and corals are observed at shallow depths in the sub-Antarctic (~300 m), while coral populations at greater depths and further south diminished. Our ecological and geochemical data indicate that habitat shifts were dictated by (i) a northward migration of food supply (primary production) into the Subantarctic Zone and (ii) poorly oxygenated seawater at depth during this Antarctic cooling interval.

1 Introduction

The rise in atmospheric CO_2 during the last deglaciation (18 to 11.5 ka) occurred primarily during Henrich Stadial 1 (HS1; 18 to 14.7 ka) and the Younger Dryas (YD; 13 to 11.5 ka) intervals that were associated with high-latitude cooling in the northern hemisphere and warming in the south. These CO_2 increases, each of more than 40 ppm, were separated by a ~1500-year interval known as the Antarctic Cold Reversal (ACR), where the deglacial rise in CO_2 stalled and Antarctic temperatures cooled (Figure 1A; (Bereiter et al., 2014; Blunier et al., 1997; Parrenin et al., 2013)). The effects of the ACR have been documented in paleo-temperature records as far afield as 40°S, thus this enigmatic pause in the deglaciation and the associated changes in the Southern Ocean have drawn much attention (Pedro et al., 2016; Putnam et al., 2010).

This article is protected by copyright. All rights reserved.

Accepted Article

The Southern Ocean surrounding Antarctica is a region where carbon- and nutrient-rich deep waters are upwelled (Figure 2), with the strength and position of the upwelling controlled by sea ice and wind stress (Ferrari et al., 2014; Menviel et al., 2018). Expansive sea ice during the Last Glacial Maximum (LGM) likely presented a physical barrier to air-sea gas exchange in the Southern Ocean (Stephens and Keeling, 2000) and changed the large scale geometry of the overturning circulation (Ferrari et al., 2014), giving rise to poorly oxygenated bottom waters (Jaccard et al., 2016), and greater carbon storage at depth (Rae et al., 2018). As Antarctica warmed during HS1 and the YD and sea ice retreated, the westerly winds shifted southward causing intensified upwelling in the Antarctic Zone, stimulating high primary productivity (Figure 1F), and releasing these deep carbon stores (Anderson et al., 2009). By contrast the ACR cooling was associated with a resurgence of Antarctic sea ice extent as evidenced by concentrations of wind-blown sea-salt within Antarctic ice cores (ssNa; Figure 1A; (Buizert et al., 2015)), a resurgence of *Fragilariopsis curta* and *F. cylindrus* abundance within Antarctic Zone diatom assemblages (Figure 1E; (Bianchi and Gersonde, 2004), and climate modelling (Lowry et al., 2019). Furthermore, enhanced sea ice would have shifted the position of the westerlies northward (McCulloch et al., 2000). Correspondingly, there is some evidence of higher primary productivity in the Subantarctic Zone as fronts shift north, including a notable peak in total organic carbon mass accumulation rates on the Falkland Plateau (Core GC528; Figure 1D (Roberts et al., 2017)) and more subtle pauses in the deglacial decline in opal flux and nitrate utilisation at this time (Anderson et al., 2014; Martínez-García et al., 2014). Yet, despite the many records documenting changes in primary production (Anderson et al., 2002; Martínez-García et al., 2014) and shifts towards surface water biotic assemblages adapted to cooler conditions (Figure 1C & E; (Barker et al., 2009; Bianchi and Gersonde, 2004)), relatively little is known about associated impact on benthic marine organisms in the Southern Ocean during the ACR.

With their important roles in carbon-cycling and deep-sea food webs (Gooday et al., 1992) and the creation of habitat for biodiversity hotspots (Hovland, 2008; Roberts et al., 2006), the distribution of benthic foraminifera and cold-water corals in the past are of high paleoceanographic significance. Benthic foraminiferal assemblage data also

This article is protected by copyright. All rights reserved.

Accepted Article

harbour a great deal of paleoenvironmental information as different species bear an affinity to particular environmental conditions (e.g. flux of raining organic carbon or oxygen content of seawater (Gooday, 2003)). Cold-water coral habitat migration has been previously suggested at ~50°S during the ACR in the Drake Passage (Margolin et al., 2014) and Tasmania (Thiagarajan et al., 2013), yet these studies were based on limited coral specimens and low precision dating techniques. Furthermore, without paired geochemical proxy data, the dominant drivers of any changes in benthic ecology remain unclear (e.g. circulation driven primary production and food supply, dissolved oxygen, seawater pH).

Cold-water corals offer a variety of paleoceanographic proxy potential, including tracers for circulation, productivity, and seawater pH. Radiocarbon data, for instance, can be corrected for post-mortal decay using uranium-thorium dating, and used to reconstruct changes in seawater ventilation. Published radiocarbon data from Tasmania Seamounts and Drake Passage corals (Hines et al., 2015; Li et al., 2020) suggest that initial destratification of the Southern Ocean during HS1 halted briefly during maximum Antarctic cooling in the late ACR (~13.5 ka). Ba/Ca ratios in cold-water corals record the dissolved barium concentration in seawater ($[Ba]_{sw}$; (Anagnostou et al., 2011; Spooner et al., 2018)), which is controlled by adsorption/absorption onto organic particulates in the upper ocean and release during remineralisation at depth (Cardinal et al., 2005), resulting in a nutrient-like seawater profile (Chan et al., 1977). Ba/Ca data may thus provide insights into changes in upwelling of deep waters and/or surface primary productivity that may act as a food source for benthic ecosystems. The boron isotopic composition ($^{11}B/^{10}B$ ratio expressed as $\delta^{11}B$ relative to NIST SRM 951 in parts per thousand) of cold-water corals increases as a function of seawater pH and has been used to document carbon release from the deep Southern Ocean during the last deglaciation (Rae et al., 2018). Coral $\delta^{11}B$ data can therefore be used to assess whether large changes in pH (and associated shifts in saturation state) were responsible for changes in benthic calcifier abundance.

Here we use well-dated biotic and paleoceanographic records to answer the questions (1) What impact did a return to more glaciated conditions have on benthic ecology in

This article is protected by copyright. All rights reserved.

Accepted Article

the Southern Ocean during the ACR? (2) What were the primary drivers of deep-water habitat changes for marine calcifiers? We provide new benthic foraminifera and cold-water scleractinian coral abundance data and geochemical reconstructions from sites across the Drake Passage, spanning the Antarctic, Polar Front and Subantarctic Zones and occuping water depths from 300 to 1750 m (Figure 2). More than 600 new coral radiometric dates have been added to initial coral abundance compilations (Burke et al., 2010; Margolin et al., 2014) and many low precision "reconnaissance" dates have now been improved by isotope dilution U-Th techniques (see methods). These new data allow us to present precisely-dated, coral abundance data from across the Drake Passage. Furthermore, we provide new records of productivity and pH from coral Ba/Ca and $\delta^{11}B$ measurements for direct comparison with published coral geochemical records (Burke and Robinson, 2012; Chen et al., 2015; Li et al., 2020). When viewed in conjunction with benthic foraminifera assemblage data, these results provide unique insight into the likely causes of biotic change during the ACR.

2 Methodology

2.1 Benthic foraminifera assemblage counts

Sediment core GC528 (53.01°S, 58.04°W, 598 m water depth) was collected on Cruise JR244 from the Falkland Plateau within the Subantarctic Zone (approximately 150 km north of Burdwood Bank; Figure 2); a site currently bathed in Antarctic Intermediate Water. We adopt the radiocarbon-based age model for this core from Roberts et al. (2016). This includes 14 radiocarbon measurements of *Uvigerina bifurcata* between 66 and 229 cm core depth (11 to 18 ka) with ^{14}C reservoir corrections based on nearby coral measurements by Burke and Robinson (2012). The benthic foraminiferal assemblage was determined on the >63 μm size fraction of 218 core samples. This broad size fraction was targeted so as to include the smaller *Alabaminella weddellensis* and *Epistominella exigua* species in count data (Gooday, 1993). A minimum of 300 individuals were counted per sample; samples containing significantly more than 600 individuals were split. Correspondence Analysis of count data between 8 and 22 ka (54 and 321 cm core depth) was conducted to establish the contrasting assemblages before,

This article is protected by copyright. All rights reserved.

during, and after the ACR. One sample within a suspected dissolution horizon at 19 ka (see Section 4.1.1) dominated by agglutinated foraminifera (~80%) was omitted to remove its weighting on axes.

2.2 Cold-water coral abundance

Fossil cold-water scleractinia were collected from Shackleton Fracture Zone (60.2°S, 57.8°W), Sars Seamount (59.7°S, 68.8°W), Interim Seamount (60.6°S, 66.0°W), Cape Horn (57.2°S, 67.0°W) and Burdwood Bank (54.7°S, 62.2°W) during Research Cruises LMG06-05, NBP0805 and NBP1103 (Figure 2). Most corals were collected the using dredges (reinforced box dredge) and trawls (Blake and Otter). A select few corals were collected by gravity core at Burdwood Bank; the age-depth distribution of these samples suggests that the relatively shallow depth of dredging does not unduly bias sampling (Margolin et al., 2014).

Today, Shackleton Fracture Zone lies south of the Polar Front in the Antarctic Zone, Sars and Interim Seamounts are located in the Polar Front Zone, and Cape Horn and Burdwood Bank are in the more northerly Subantarctic Zone (Figure 2). The shallowest coral samples come from depths of 334 m on Burdwood Bank that are currently bathed in Subantarctic Mode Waters. Corals were also collected at Burdwood Bank from 700 to 1520 m, at water depths corresponding to modern day Antarctic Intermediate Water. Corals recovered from depths 695 to 1200 m further south at Sars Seamount are currently bathed in Upper Circumpolar Deep Water while deeper samples at this site sit within Lower Circumpolar Deep Water (1300 to 1750 m). Samples from the nearby Interim Seamount are grouped with Sars samples for the purposes of this discussion.

More than 1500 coral samples were initially "reconnaissance" dated by radiocarbon and U-series laser ablation techniques (typically ±650 years age control; this study and published data from (Burke et al., 2010; Margolin et al., 2014; Spooner et al., 2016)). This technique is based solely on measured $^{230}Th/^{238}U$ ratios and therefore must assume that the initial $^{234}U/^{238}U$ of the sample is similar to modern seawater and that the initial ^{230}Th is negligible (Spooner et al., 2016). Previous age distribution assessments from these sites by Margolin et al. (2014) only included around half the number of specimens

This article is protected by copyright. All rights reserved.

Accepted Article

Accepted Article

in our study and of those only 59 had high-precision dates (Burke and Robinson, 2012), thus interpretations of benthic population changes were heavily reliant on these less precise reconnaissance dates – with the age resolution being similar to the duration of the ACR. Since those initial studies, where sufficient well-preserved material permitted, deglacial age samples have been precisely dated using U-Th isotope-dilution techniques (Chen et al., 2015; Cheng et al., 2000), typically offering age uncertainties better than ±250 years for deglacial aged samples (2 SD). This study includes 604 corals newly dated by "reconnaissance" techniques and a further 124 new high precision isotope-dilution dates that are combined with previous coral dating studies (Burke and Robinson, 2012; Chen et al., 2015; Li et al., 2020). The result is that more than 47% of these coral samples within the deglacial interval now have precise dates. While reconnaissance dates are still shown for samples that lack precise dates in coral abundance plots, the vast majority of specimens used for $\delta^{11}B$ and Ba/Ca records have precise dates assigned by isotope-dilution techniques.

2.3 Cold-water coral Ba/Ca and $\delta^{11}B$ analyses

Deglacial coral samples from Burdwood Bank and Sars/Interim Seamounts were selected for Ba/Ca analysis to examine changes in circulation and organic matter flux within the Subantarctic and Polar Front Zones (water depth range: 300 to 1750 m). The Burdwood Bank site, with coral samples present during the late ACR, was primarily targeted for boron isotope analysis in this study. These new $\delta^{11}B$ data are supplemented by existing data from Sars/Interim sites (Rae et al., 2018), to which we add one new boron isotope measurement from a newly dated coral from Interim Seamount (13.6 ka; late ACR). Whole "S1" septa and attached theca were taken from cup corals using a rotary cutting tool for geochemical analysis. This tool was further used to remove surficial oxide coatings and any chalky white altered carbonate. This type of visual inspection and physical removal of diagenetically altered material from deglacial specimens is shown to yield robust U isotope results reducing the effects of open-system behavior (Burke and Robinson, 2012; Chen et al., 2016). Microstructures within cold-water corals are known to exhibit highly-contrasting trace metal and boron isotopes values (Blamart et al., 2007; Gagnon et al., 2007; Stewart et al., 2016),

This article is protected by copyright. All rights reserved.

Accepted Article

therefore where sufficient sample material allowed, multiple sub-samples (typically duplicates) were measured to characterize microstructural bias. Coral fragments were finely crushed using a pestle and mortar before a 5 mg aliquot of the homogenous powder was taken. A warm 1% H_2O_2 (buffered in NH_4OH) oxidative clean and weak acid polish (0.0005 M HNO_3) was performed on powders (Boyle, 1981; Rae et al., 2011). Samples were then dissolved in distilled 0.5 M HNO_3.

All coral trace metal and boron isotope analyses were carried out at the Universities of Bristol or St Andrews. An aliquot of the dissolved sample was analyzed by ICP-MS using well-characterised, matrix-matched, synthetic standard solutions to give Ba/Ca ratios. Repeat analysis of NIST RM 8301 (Coral) (n=19) yielded analytical precision of <±2 % (2 SD). Small analytical offsets between the labs are quantified and corrected using NIST RM 8301 (Coral) results to bring values into line with interlaboratory comparison results following (Stewart et al., 2020). To this end, Ba/Ca ratios of samples measured in Bristol and St Andrews were adjusted by 0.95 and 1.03 respectively.

For boron isotope analysis, a further aliquot of the dissolved sample containing ~40 ng B was separated from the carbonate matrix using 20 µl Amberlite IRA 743 boron-specific anionic exchange resin micro-columns (Foster, 2008). The $\delta^{11}B$ of purified boron samples were measured by (MC)-ICPMS against NIST SRM 951 at Bristol and St Andrews following identical protocols (Foster, 2008; Rae et al., 2018; Rae et al., 2011). Interlaboratory comparison studies reveal no systematic analytical offset between these institutions or other laboratories using this method (Gutjahr et al., 2020; Stewart et al., 2020). Samples, blanks, and standards were introduced to the instrument in a 0.5 M HNO_3 and 0.3 M HF acid matrix to aid B wash out (Zeebe and Rae, 2020). Full procedural uncertainty is assessed using repeat measurements of NIST RM 8301 (Coral) consistency standard (Stewart et al., 2020) yielding average $\delta^{11}B$ values of 24.24 ± 0.15‰ at Bristol (2 SD; n=67) and 24.12 ± 0.12‰ at St Andrews (2 SD; n=15). Total procedural blanks (n=21) were on average <0.13% of the sample boron loaded onto columns.

This article is protected by copyright. All rights reserved.

Accepted Article

2.4 Estimating seawater [Ba] and pH

Seawater barium concentration ($[Ba]_{sw}$; nmol/kg) is estimated from coral Ba/Ca using the cold-water coral calibration of Spooner et al. (2018) (Equation 2). Many of the modern corals included in the Spooner et al. (2018) calibration are from the same sites used in our study.

$$\text{Ba/Ca (μmol/mol)} = 0.15[\pm0.02] \times [Ba]_{sw} + 2.5[\pm1.4] \quad (2)$$

Scleractinian corals do not make their carbonate skeleton from ions derived directly from seawater, rather they calcify from a semi-restricted extracellular calcification fluid (Al-Horani et al., 2003). The chemistry of this calcification fluid is modified through ion pumping mechanisms (Ca-ATPase pump) that transport in Ca^{2+} ions at the expense of H^+ to make conditions more favourable for calcification. This "pH up-regulation" means that internal pH is routinely higher (~ pH 9) than external seawater (Al-Horani et al., 2003; Gagnon et al., 2021). This results in coral $\delta^{11}B$ values that are higher (cold-water corals ~+11‰ higher; (McCulloch et al., 2012)) than that predicted by the simplified relationship between $\delta^{11}B_{borate}$ and seawater pH described Equation 3 (Zeebe and Wolf-Gladrow, 2001); see also full expression in Rae (2018):

$$\text{pH} = \text{p}K_B^* - \log\left(-\frac{\delta^{11}B_{sw} - \delta^{11}B_{borate}}{\delta^{11}B_{sw} - \alpha_B\delta^{11}B_{borate} - 1000(\alpha_B - 1)}\right) \quad (3)$$

where α_B (1.027) is the fractionation factor between boric acid and borate (Klochko et al., 2006), $\delta^{11}B_{sw}$ (39.61) is the $\delta^{11}B$ of seawater (Foster et al., 2010) and pK_B^* is the dissociation constant of the two boron species (8.82 for temperature salinity and pressure of 3°C, 35 psu, and 1000 m respectively, typical of sites in this study).

Scleractinian coral $\delta^{11}B$ varies as a function of ambient seawater pH, providing the basis for deep water pH reconstruction from these archives (Rae et al., 2018). A secondary influence of dissolved inorganic carbon on coral $\delta^{11}B$ has also been observed in culture, that has the same sense of change as pH, with lower pH, carbon-rich waters yielding lower $\delta^{11}B$ (Gagnon et al., 2021). Due to biological vital effects, taxa-specific coral $\delta^{11}B$ vs pH calibrations are required to give seawater pH estimates (Anagnostou et al., 2012; Martin et al., 2016; McCulloch et al., 2012; Stewart et al., 2016). Cold-

This article is protected by copyright. All rights reserved.

Accepted Article

water coral samples used in this study include *Desmophyllum, Flabellum, Caryophyllia and Balanophyllia*. Calibrations for *Desmophyllum dianthus* and *Caryophyllia smithii* (Anagnostou et al., 2012; McCulloch et al., 2012; Rae et al., 2018) reveal that these taxa (both Family Caryophylliidae) upregulate internal pH by a similar amount and broadly lie on a common calibration line (Supplementary information). By contrast, *Balanophyllia* cultured under laboratory conditions yield similar δ^{11}B-pH sensitivity (slope of regression) to the well-studied taxon *Desmophyllum*, but with δ^{11}B values approximately 1.5‰ lower for a given seawater pH (Gagnon et al., 2021) (Supplementary information). In light of these contrasting vital effects and the additional minor dependency of coral δ^{11}B on dissolved inorganic carbon, in this study we adopt a simple approach to our assessment of relative changes in seawater pH, presenting raw coral δ^{11}B, but with a +1.5‰ adjustment factor applied to *Balanophyllia* δ^{11}B results (all figures and discussion of *Balanophyllia* δ^{11}B refer to adjusted values).

3 Results

3.1 Benthic ecology during the ACR

3.1.1 Benthic foraminifera

Our deglacial benthic foraminiferal assemblage data from core GC528 are shown in Figure 3. Both percentage (Figure 3A) and raw benthic foraminiferal abundance count data (Figure 3B, C, D) from this core suggest that three taxa dominate the assemblage at different times during the deglaciation: *Fursenkoina fusiformis* prior to the ACR (~80%; 22 to 14.5 ka), *Uvigerina bifurcata* during the ACR (~80%; 14.5 to 13 ka), and *Epistominella exigua* after the ACR (~30%; 13 to 8 ka). The ACR also features several short-lived (<100-year duration) peaks in abundance of *E. exigua* (Figure 3D). The peak in relative abundance of thick-walled infaunal foraminifer *Uvigerina* during the ACR (Figure 3C) is coincident with the peak in total organic carbon (TOC) mass accumulation rates in the same core (Figure 1D; (Roberts et al., 2017)), and with higher total benthic foraminiferal abundance (Figure 3E) and diversity (Figure 3F) compared to the preceding HS1 event (~16 ka).

This article is protected by copyright. All rights reserved.

Accepted Article

We confirm these inferred deglacial shifts in foraminiferal assemblage through a Correspondence Analysis approach (Figure 4). Once results were plotted on their principal axes, broad groupings were defined that encompass >95% of the respective age points (pre-, during-, and post-ACR) and their neighbouring taxa. While there is some overlap between assemblages, the broad-scale assemblage shifts from before (Assemblage 1 dominated by *F. fusiformis*; 22 to 14.5 ka), during (Assemblage 2 dominated by *U. bifurcata*; 14.5 to 13 ka), and after (Assemblage 3 dominated by *E. exigua*; 13 to 8 ka) the ACR appear robust (Figure 4). Alternatively, when plotted over time, the shift in sign (negative to positive) of principal component 1 (Axis 1) shows that the majority of the variance in the benthic foraminiferal data is described by a shift from Assemblage 1 to Assemblage 3 during the deglaciation (Figure 3G). The negative shift in principal component 2 (Axis 2) during the ACR interval shows that the next most important change in assemblage was a shift from Assemblages 1 and 3 to Assemblage 2 at approximately 14 ka (Figure 3H).

3.1.2 Cold-water corals

Our new radiometric dates for Drake Passage cold-water corals are shown in Figure 5 (A to D). Once these data are combined with previously published dates, grouped by depth interval, and plotted as histograms, changes in coral abundance over time become clear (Figure 6). Similar to *Uvigerina* abundance, we observe a peak in coral (absolute) abundance at ~300 m water depth at the nearby Burdwood Bank site during the ACR (Figure 6A), where the genus *Balanophyllia* dominates the assemblage (74% of individuals; Supplementary material). By contrast, at deeper depths (>700 m) on Burdwood Bank, we see a distinct demise in coral populations, identified by a gap in occurrence (Figure 6A), with no recovered corals dated between the ages of 14 and 13.2 ka despite dedicated analytical effort. With *Balanophyllia* also present at deeper depths both before and after this gap in occurrence, this event appears to have impacted all coral genera (Supplementary material). A similar decrease in coral abundance also occurs across the Cape Horn, Sars/Interim Seamount, and Shackleton Fracture Zone sites with just 10 corals found within this entire 800-year interval (Figure 6B, C and D). With a greater number of coral specimens recovered from Cape Horn and

This article is protected by copyright. All rights reserved.

Accepted Article

Sars/Interim sites, a clear decrease in coral abundance is observable from the peak in abundance at the end of HS1 (14.5 ka; up to 15 individuals per 200 yr bin of the histograms) to near zero by the middle of the ACR. At the Sars/Interim sites, coral numbers recover initially at the deeper sites (~12 ka), followed by a return of shallower water specimens later in the YD (~11.5 ka; Figure 6C).

We adopt a statistical approach to assess the likelihood that the 800-year gap in coral occurrence during the late ACR (14.0 to 13.2 ka) is merely an artefact of sampling. 310 corals were recovered from deep waters (>500 m) at all sites with ages between 16.0 and 11.5 ka (late HS1, ACR and YD intervals). We run multiple Monte Carlo simulations (10,000) to estimate the probability that a random distribution of these corals would yield 10 or fewer corals within any 800-year interval between 16.0 and 11.5 ka. In more than 99% of simulations there were more than 10 corals in 800-year bins suggesting that the gap in coral occurrence is unlikely a sampling artefact. This result is robust (95% confidence) even if we limit the sample set to only the most well-dated corals in this interval (age uncertainty <±400 years; n=158; i.e. isotope-dilution dates and only the best laser reconnaissance analyses) and include those samples that fall within age uncertainty of the ACR gap.

3.2 Coral geochemical records

Replicate Ba/Ca measurements in these corals generally agreed within 5% of one another, thus internal skeletal variability in Ba has little influence on our record (Figure 5E). Mean Ba/Ca ratios in corals from both deep and shallower depths at the Sars/Interim Seamount sites are generally high (>15 µmol/mol) during the YD and HS1 (Figure 7D), equating to $[Ba]_{sw}$ values comparable with modern measurements at these sites (~100 nmol/kg; (Spooner et al., 2018)). We find similarly high Ba/Ca ratios in the few Sars samples available in the early and latest ACR (i.e. outside of the occurrence "gap"). Samples from Burdwood Bank have generally lower Ba/Ca ratios (~10 µmol/mol) in both shallow and deep waters throughout the deglacial interval, with the exception being corals at ~300 m within the latter part of ACR interval (~13.3 ka), and

This article is protected by copyright. All rights reserved.

one coral at ~14 ka that lived at 1400 m depth, exhibiting Ba/Ca values similar to those at the more southerly deep Drake Passage sites (~20 µmol/mol; $[Ba]_{sw}$ ~120 nmol/kg).

The majority of our $\delta^{11}B$ replicates from the same coral fall within 0.5 ‰ of one another, though some samples have higher variability (~1 ‰; Figure 5F). Average $\delta^{11}B$ measurements from corals are generally high (>26 ‰) during the initial phase of the ACR (~13.8 to 14.6 ka), including our new data from Burdwood Bank and new and published data from the Sars/Interim Seamount sites ((Rae et al., 2018); Figure 7E). During the latter half of the ACR (~13.2 to 13.8 ka), at the same time as the coral abundance gap at depth and the Ba/Ca peak in Burdwood Bank samples, there is some hint of lower or more variable values. We also note that a single *Desmophyllum* sample at 16.3 ka records low $\delta^{11}B$ (<25‰, inferred seawater pH < 7.7; Figure 7E), similar to the low $\delta^{11}B$ excursions at the Sars/Interim Seamounts at the end of YD and HS1 (14.7 and 11.5 ka; (Rae et al., 2018)). As this event is represented by a single coral we refrain from using it in a detailed discussion, however we note that it has a temporal correspondence with the 16.3 ka centennial CO_2 rise event (Marcott et al., 2014) and the associated Southern Ocean ventilation anomalies revealed by coral radiocarbon in Li et al. (2020).

4 Discussion

By combining records of multi-faunal biotic change and coral geochemistry during the last deglaciation we seek to come to a consensus view of the both the timing of benthic habitat change in the Southern Ocean and its potential paleoceanographic drivers. In this discussion we first reason that recorded shifts in benthic foraminiferal assemblage are a true representation of faunal exchange and are not merely a result of variable preservation in core GC528. Secondly, we argue that peaks in *Uvigerina bifurcata* and shallow cold-water abundance in the Subantarctic Zone during the ACR are the result of the northward shift in centres of primary production. Finally, by considering all evidence from benthic foraminiferal abundance and coral geochemistry datasets we posit that depletion of oxygen in seawater was the principal cause of the disappearance of corals at deeper and more southerly Drake Passage sites during the ACR.

This article is protected by copyright. All rights reserved.

Accepted Article

Accepted Article

4.1 Benthic foraminiferal assemblage and primary productivity

4.1.1 Preservation bias

Benthic foraminiferal assemblage data have the potential to be biased by variable preservation. Thin-walled specimens are more vulnerable to dissolution compared to thick-walled taxa; thus, a dissolution interval can lead to an increase in the proportion thick-walled benthic foraminifera within the fossil assemblage, without an actual increase in their true abundance within the living population at that time. An example of a potential dissolution event is present in GC525 at ~19 ka where a peak in the percentage of the thick-walled taxon *U. bifurcata* (Figure 3A) occurs during a low in total benthic foraminiferal abundance and diversity (Figure 3E and F) and is not associated with a peak in *U. bifurcata* abundance per gram (Figure 3C). The proportion of non-calcareous, agglutinated, foraminifera is also high within this interval, further supporting a transient carbonate dissolution event. By contrast, the general assemblage shift from *F. fusiformis* dominated before the ACR, to *U. bifurcata* dominated during ACR, and *E. exigua* dominated after the ACR observed from relative benthic foraminiferal abundance data (Figure 3A) is also robust in the absolute counts (Figure 3B, C, D). Moreover, the double peak in *U. bifurcata* abundance during the ACR occurs during maxima in benthic foraminiferal total abundance and diversity. This result suggests that these wholescale shifts in foraminiferal abundance are not an artefact of variable preservation and that the ACR represents a true increase in abundance of *Uvigerina*.

4.1.2 Deglacial benthic foraminiferal abundance

The changes in benthic foraminifera we document in GC528 from *F. fusiformis*, to *U. bifurcata*, to *E. exigua* dominated assemblages before, during, and after the ACR respectively, are likely to represent distinct regional transitions of organic carbon flux to the seafloor, impacting benthic ecology. On the West Antarctic Peninsula shelf the species *F. fusiformis* is typically associated with high primary productivity resulting from seasonal ice melt (Peck et al., 2015). High *F. fusiformis* abundance on the Falkland Plateau during HS1 and LGM likely represents seasonal productivity peaks

This article is protected by copyright. All rights reserved.

Accepted Article

associated with nutrient-rich meltwater injections and/or seasonal sea ice melt. In shelf settings such as this, the genus *Uvigerina* is also associated with high primary productivity regimes (100 to 300 g m^{-2} yr^{-1}) where organic carbon fluxes to the seafloor are elevated (2 to 20 g m^{-2} yr^{-1}) (Gooday, 2003). *Uvigerina* are also able to withstand lower oxygen conditions owing to its ability to denitrify (Piña-Ochoa et al., 2010). As a thick-walled foraminifer resistant to winnowing by currents, *Uvigerina* is also found in high relative abundance in strong flow speed environments, with *U. bifurcata* in particular associated with the Falkland Current (Harloff and Mackensen, 1997). Within GC528, the close association of *U. bifurcata* with high TOC mass accumulation rates (Figure 1D) and increases in the $\delta^{13}C$ and C/N ratios of TOC (Roberts et al., 2017), suggests that the shift to Assemblage 2 is most likely a result of northward displacement of centres of surface-water primary production into this region and potentially enhanced current speeds across on the Falkland Plateau during the ACR. Furthermore, this interpretation is consistent with the transient peaks in *E. exigua* also seen at this time: *E. exigua* is classed as an opportunist species adapted to fluctuating nutrient supply and preferring strong seasonality in open ocean waters (Barker et al., 2009; Gooday, 1993). These interludes of *E. exigua* abundance may therefore also support claims that the ACR was a time of enhanced seasonality in Southern Ocean sea ice extent (Fogwill et al., 2020). The abrupt decline in *U. bifurcata* at ~13 ka suggests a rapid transition at the end of the ACR from an extremely high primary productivity regime on the Falkland Plateau to conditions approaching the modern.

4.2 Controls on cold-water coral abundance

4.2.1 Shallow Subantarctic Zone corals

We explore the possibility that the peak in *Balanophyllia* coral abundance at shallow depths on Burdwood Bank during the ACR may be linked to upwelling and plentiful food supply caused by a shift in Polar Front position towards the Subantarctic Zone. The rain of organic carbon through the water column is an important food source for all benthic marine calcifiers that live outside of the photic zone, not least cold-water corals (Roberts et al., 2006). The coral *Balanophyllia* in particular has been shown to maintain calcification and respiration rates, even under low pH conditions (such as

This article is protected by copyright. All rights reserved.

Accepted Article

those in the Southern Ocean), provided that food supply is high (Crook et al., 2013; Griffiths et al., 2019).

The abundant *Balanophyllia* corals living at shallow depths on Burdwood Bank between 13.8 and 13 ka also exhibit anomalously high Ba/Ca ratios. With supporting evidence for locally high productivity (e.g. our benthic foraminiferal assemblage data), it is possible that seafloor [Ba] was enhanced by a high flux of Ba-rich (organic) particulates during the ACR. Ba is actively scavenged from seawater as a result of barite formation down to 1000 m water depth (Stroobants et al., 1991), hence high particulate organic flux to the sea floor has the potential to reduce seawater [Ba] at these relatively shallow water depths (~300 m). However, it is not uncommon for upwelling of Ba-rich deep waters to overwhelm any depletion caused by scavenging (Montaggioni et al., 2006). Therefore, the increase in Ba/Ca values measured in these shallow corals, to values more typical of deeper / more poleward sites, suggests that shallow Burdwood Bank was influenced by upwelling of deeper, high-[Ba] deep waters during the late ACR. We consider it likely therefore, that the increased coral abundance (notably of *Balanophyllia*) at ~300 m water depth at Burdwood Bank, along with the shift in benthic foraminifera assemblages on the Falkland Plateau, result from higher productivity driven by increased nutrient availability. Furthermore, the shift towards a *Uvigerina* dominated assemblage and evidence from sortable silt from core GC528 suggest that there was an increase in flow of water from the Pacific through the Drake Passage after 14 ka (Roberts et al., 2017). This strengthening of the bottom current would be consistent with enhanced regional upwelling and corals may have further benefited from optimal bottom current speeds for larval transport or prey capture (Purser et al., 2014).

We posit that changes in benthic ecology we document in the Drake Passage are unlikely a local effect and were seen throughout the Southern Ocean. In contrast to the high TOC flux in the Subantarctic Zone (Roberts et al., 2017), decreases in opal (Figure 1F; (Anderson et al., 2009)) and biogenic barium flux (Figure 1G; (Jaccard et al., 2016)) in the Antarctic Zone suggest that primary production decreased at more poleward sites during the ACR. This anticorrelation between peaks in organic matter /

This article is protected by copyright. All rights reserved.

Accepted Article

barium fluxes between sites north and south of the polar front forms the basis of the theory that the focus of primary production was displaced northward during Antarctic cool periods as a result of expanding sea ice (Anderson et al., 2002), an equatorward shift in the Southern Hemisphere westerly winds (Toggweiler, 2009), and the associated changes in buoyancy flux (Watson and Naveira Garabato, 2006). An increase in coral abundance similar to that we observe at Burdwood Bank is also seen at the shallowest sites on the Tasmanian Seamounts in the South Pacific (~1600 m; ~45°S) between 13.5 and 14.5 ka (Thiagarajan et al., 2013). Synchronous increases in cold-water coral abundance in opposing sectors of the Southern Ocean therefore suggest that these changes in benthic ecology are the result of the wholesale displacement of the Polar Front northward.

Our benthic ecological records provide yet more evidence that centres of primary production moved further from the pole during the ACR. This result however makes the source of a transient peak in marine-aerosol fluorescent organic matter biomarkers (derived from nanoplankton, picoplankton and picoeukaryotes) recorded in the Patriot Hills ice core on West Antarctica during this interval rather enigmatic (Figure 1B; (Fogwill et al., 2020)). To explain the occurrence of an organic-rich zone within this ice-core, we suggest that marine-derived organics were likely sourced from the more distal Subantarctic Zone where productivity was high (rather than the immediate Antarctic Zone) or that marine aerosols in polar regions were simply more efficiently transported to the Patriot Hills during interval the ACR interval of cooling (e.g. (Markle et al., 2018)).

4.2.2 Deep-dwelling and Polar Front Zone corals

While the increased Subantarctic Zone primary productivity appears to favour shallow cold-water coral habitats at the ACR, we find a distinct minimum in coral abundance in the late ACR at deeper depths on Burdwood Bank, as well as across all depths at the more southerly Sars/Interim sites. In the following section we show that our coral $\delta^{11}B$ records reveal little evidence for large reductions in seawater pH during the ACR, and

This article is protected by copyright. All rights reserved.

Accepted Article

instead we suggest that low oxygen conditions were more likely responsible for the temporary loss of these cold-water coral habitat.

High surface water primary production recorded during the ACR at the shallow Burdwood Bank coral and sediment core sites allows us to discount food supply as a limiting factor for coral occurrence at the deep Burdwood Bank site. In addition to food supply however, it is thought that cold-water scleractinian corals tend to live in seawater that is near to or above the aragonite saturation depth ($\Omega > 0.9$) (Guinotte et al., 2006; Thiagarajan et al., 2013) and which has dissolved oxygen content greater than ~165 µmol/kg (Dodds et al., 2007; Thiagarajan et al., 2013). The individual impact of multiple stressors on cold-water coral physiology is difficult to establish, particularly for ancient samples (Gori et al., 2016). However, it seems unlikely that a decrease in saturation state is the leading control on the absence of corals in deeper, more southerly sites during the ACR. Although the coral gap precludes detailed $\delta^{11}B$-based assessment of pH at this time, the one available datum at ~13.6 ka from Interim Seamount shows relatively high $\delta^{11}B$ values. Furthermore, previous $\delta^{11}B$ reconstructions show that Southern Ocean cold-water corals can, to some extent, tolerate low pH conditions, for example during the LGM and during centennial-scale events during the last deglaciation (Rae et al., 2018). We note also that the high Ba values in shallow Burdwood Bank *Balanophyllia* in the early ACR are associated with relatively high $\delta^{11}B$, suggesting some decoupling of Ba and carbonate chemistry. This might result from the relatively deep regeneration profile of Ba, and/or from a combination of high Ba and buffering of pH by carbonate dissolution in waters input from the Pacific, so although the Ba data suggest high availability of nutrients this does not necessarily imply the influence of carbon-rich (low pH) waters from depth. Whatever the exact explanation, as there are no low $\delta^{11}B$ values (e.g. <25 ‰) recorded in available samples during the late ACR we infer that any decrease in pH associated with a northward shift in organic matter flux was likely modest and within the uncertainty of bulk coral $\delta^{11}B$-pH proxy capabilities (i.e. <0.2 pH units; (Anagnostou et al., 2012; Stewart et al., 2016)). We therefore suggest that low pH and saturation state may not have been the dominant factor limiting deep and southerly coral growth during the late ACR.

This article is protected by copyright. All rights reserved.

Accepted Article

In lieu of large changes in pH or saturation state, we draw on several lines of evidence for regionally low oxygen conditions at this time. The thick-walled shallow infaunal *Uvigerina* genus is readily abundant in low oxygen bottom water conditions (Boersma, 1986; Kaiho, 1994) and is often found to dominate in oxygen minimum zones (Kender et al., 2019; Schumacher et al., 2007). The shift towards a *Uvigerina* dominated assemblage during the ACR on the Falkland Plateau is therefore suggestive of high primary productivity and is consistent with low dissolved oxygen. Further evidence for a return to widespread lower oxygen conditions in the Southern Ocean region is provided by a collapse in epifaunal-infaunal (bottom water to pore water) benthic foraminiferal carbon isotope gradients during the ACR (Gottschalk et al., 2016; Haddam et al., 2020).

Many paleoceanographic records also support a regional increase in stratification of seawater that would make the Southern Ocean more prone to widespread oxygen depletion at depth. Coral radiocarbon records show an increase in B-atmosphere age (^{14}C age difference between sample and the contemporary atmosphere) caused by a relative decrease in ^{14}C at the shallowest site (~300 m) on Burdwood Bank between 14.7 to 13.5 ka (Figure 7B) towards values similar to those seen at the deeper and more southerly sites (Figure 7C) immediately before and after the ACR (Burke and Robinson, 2012; Chen et al., 2015; Li et al., 2020). This radiocarbon depletion at shallow depths further implies that this site had limited exchange with the atmosphere and was more influenced by deeper, older, waters at this time. Other lines of evidence suggest that the impacts of this return to more stratified conditions were felt far beyond the Drake Passage. There is a sharp 500-year increase in B-atmosphere age measured in corals from the Tasmania Seamounts (Figure 7A; (Hines et al., 2015)) also supporting increased isolation and influence of older waters over this time period. Stable silicon isotope ratios from the Indian Ocean show a striking increase during the ACR, indicative of enhanced silicic acid utilisation relative to supply (Dumont et al., 2020). More stratified conditions and more efficient nutrient utilisation in the polar frontal zone are also inferred from the increase in the available cold-water coral nitrogen isotope data (Figure 7F; (Li et al., 2020; Wang et al., 2017)). Furthermore, planktonic foraminiferal δ^{11}B-based surface water pH records (also from 44 °S) suggest

This article is protected by copyright. All rights reserved.

the Subantarctic Zone briefly transitioned from a net source of carbon during HS1 to a net sink between 14 and 13 ka (Martínez-Botí et al., 2015). A reduction in dissolved oxygen content of seawater is therefore a likely driver of low coral abundance at this time and was likely caused by (i) an increase in sea ice extent that decreased air-sea gas exchange at more southerly sites, and (ii) remineralization of enhanced organic carbon export to depth in the Subantarctic Zone (Figure 8; (Buizert et al., 2015; Stephens and Keeling, 2000)).

5 Conclusions

We show that significant changes in benthic ecology occurred during the Antarctic Cold Reversal within the Drake Passage (Figure 8). Increased abundance of corals, a shift towards a *Uvigerina* dominated benthic foraminifera assemblage, and elevated coral Ba/Ca ratios at more northerly and shallow sites during the ACR were most likely driven by enhanced surface water nutrient supply, primary production, and thus food supply to the benthos in the Subantarctic Zone. We also find a contemporaneous gap in coral occurrence at more southerly/deeper sites during the ACR. We suggest this loss of habitat was the result lower dissolved oxygen levels at depth facilitated by extended ice cover and seawater stratification in the Antarctic Zone. Thus, shifts in food supply and changes in oxygen content of seawater during the ACR had profound impacts on the viability of benthic habitats for marine calcifiers both north and south of the Polar Front.

6 Acknowledgements

We acknowledge the crew and researchers on board the research cruises who obtained the samples for this study. We thank C. Coath, C. Taylor, S. Mitchell, M. Prokopenko, M. Auro, A. Samperiz, M. Ferreira, C. Cole, and E. Littley for their help with laboratory work. We thank the editors and anonymous reviewers for their comments that improved this manuscript. Funding was provided by an Antarctic Bursary awarded to J.A.S., ERC and NERC grants awarded to L.F.R. (278705, NE/S001743/1,

This article is protected by copyright. All rights reserved.

Accepted Article

NE/R005117/1) and L.F.R. and J.W.B.R. (NE/N003861/1). Datasets for this research are available at https://pangaea.de/

https://doi.pangaea.de/10.1594/PANGAEA.924088 ,

https://doi.pangaea.de/10.1594/PANGAEA.924091

https://doi.pangaea.de/10.1594/PANGAEA.924097

Figure 1: Published records of biotic exchange and productivity in the Southern Ocean during the last deglacial. (**A**) Compiled and smoothed Antarctic ice core temperature change relative to modern (Parrenin et al., 2013), atmospheric CO_2 concentration (Bereiter et al., 2014)) and sea ice extent (ssNa; (Buizert et al., 2015)). Red arrows correspond to centennial-scale CO_2 rise events referred to in the text and Figure 7. (**B**) Fluorescent organic matter tryptophan-like component (fOM TRYLIS) from Patriot Hills ice core on Antarctica (Fogwill et al., 2020). (**C**) South East Atlantic planktonic foraminiferal assemblage from sediment core TN057-21 (Barker et al., 2009) for warm and cool (*Neogloboquadrina pachyderma* (sinistral) and *Turborotalita quinqueloba*) indicator taxa. (**D)** Total organic carbon mass accumulation rate of core GC528 Falkland Plateau (Roberts et al., 2017). (**E**) *Fragilariopsis curta* and *F. cylindrus* diatom abundance in core PS2090-1 (Bianchi and Gersonde, 2004). (**F**) Antarctic Zone opal flux from site TN057-13-4PC (~2800 m water depth (Anderson et al., 2009)). (**G**) Biogenic Ba flux from core TN057-13-4PC, ~2800 m water depth within the Antarctic Zone (Jaccard et al., 2016).

Figure 2: (**A**) Location of cold-water coral samples (Cruises LMG06-05, NBP0805, and NBP1103) and sediment core GC528 in the Drake Passage in this study. The position of the modern Antarctic Polar Front (purple line) is shown as the neutral density horizon of 27.9 kg/m^3 at 820 m. (**B**) Location of previously published ice core (Fogwill et al., 2020), sediment core (Anderson et al., 2009; Jaccard et al., 2016), and coral records (Hines et al., 2015) referred to in data figures. (**C**) Meridional section (yellow line in panel A), grouping of samples in this study by water depth and modern phosphate concentration and seawater pH (Olsen et al., 2016). AZ, PFZ, and SAZ denote the Antarctic, Polar Front, and Subantarctic Zones respectively.

Figure 3: Benthic foraminiferal assemblage data in this study from core GC528 Falkland Plateau (53.01°S, 58.04°W, 598 m water depth). (**A**) Benthic foraminiferal percentage abundance and (**B** to **D**) abundance per gram of sediment of dominant taxa: *Fursenkoina fusiformis, Uvigerina bifurcata,* and *Epistominella exigua*. (**E**) Total benthic foraminifera per gram of sediment. (**F**) Number of benthic foraminiferal taxa identified (measure of diversity). (**G** and **H**) Axis 1 and Axis 2 of the Correspondence Analysis (Figure 4) over time showing assemblage shifts. A potential dissolution event (~19 ka; low diversity, low total number, high proportion of thick-walled *Uvigerina*) is highlighted in yellow. This contrasts with the peak in *Uvigerina* during the ACR (~14 ka) that is associated with high total benthic foraminiferal abundance and diversity.

This article is protected by copyright. All rights reserved.

Accepted Article

Accepted Article

Figure 4: Correspondence Analysis of benthic foraminiferal assemblage data in this study from core GC528 Falkland Plateau (53.01°S, 58.04°W, 598 m water depth) for dates between 22 and 8 ka. According to their eigenvalues, Axis 1 and 2 account for >60% of the variance in the data. Crosses denote sample date factors coloured according to date before (blue), during (orange) and after (green) the ACR. Black dots denote benthic foraminiferal taxa, where the three particularly abundant taxa (Figure 3) are highlighted bold. Results show three distinct assemblages where points group by date: Assemblage 1 prior to the ACR dominated by *Fursenkoina fusiformis* (22 to 14.5 ka), Assemblage 2 during the ACR dominated by *Uvigerina bifurcata* (14.5 to 13 ka) and Assemblage 3 after the ACR dominated by *Epistominella exigua* (13 to 8 ka).

Figure 5: New radiometric dates and geochemistry of corals from the Drake Passage in this study. (**A**, **B**, **C**, **D**) Cold-water coral occurrence with depth from Burdwood Bank, Cape Horn, Sars/Interim Seamount, and Shackleton Fracture Zone respectively. Larger points are from this study. Full age distributions (outside of the deglacial interval) are shown in Supplementary Information. New coral (**E**) Ba/Ca and (**F**) $\delta^{11}B$ results in this study. Symbol shape in panels E and F denotes coral genus with *Balanophyllia* $\delta^{11}B$ data adjusted by +1.5‰ (see methods). Error bars show 2σ age uncertainties.

Figure 6: Age distribution of Drake Passage corals arranged by water depth for (**A**) Burdwood Bank, (**B**) Cape Horn, (**C**) Sars/Interim Seamounts and (**D**) Shackleton Fracture Zone sites. Histograms include all coral radiometric ages, both from this study and published results (Burke and Robinson, 2012; Chen et al., 2015; Li et al., 2020; Margolin et al., 2014).

Figure 7: Chemistry of fossil Southern Ocean cold-water corals from the last deglacial. (**A**) Benthic to contemporary atmosphere ^{14}C age offset (B-atmosphere) recorded in corals south of Tasmania (Hines et al., 2015) and **(B** and **C**) Drake Passage corals used in this study (Burke and Robinson, 2012; Chen et al., 2015; Li et al., 2020). For clarity radiocarbon error ellipses are not shown. (**D**) Coral Ba/Ca (This study; replicates averaged), converted to $[Ba]_{sw}$ using calibration by Spooner et al. (2018). (**E**) Coral $\delta^{11}B$ pH proxy (This study; replicates averaged; *Balanophyllia* $\delta^{11}B$ data adjusted by +1.5‰ (see methods)). Sars/Interim $\delta^{11}B$ data from Rae et al. (2018). Red arrows highlight the deglacial low $\delta^{11}B$ events (<25‰) at 16.3 (Burdwood Bank; this study), 14.7, and 11.5 ka (Sars/Interim; Rae et al. (2018)) discussed in the main text. (**F**) Nitrogen isotopes measured in corals from Sars/Interim sites (Li et al., 2020; Wang et al., 2017). Vertical green bar marks the late ACR gap in cold-water coral occurrence highlighted in Figure 6.

Figure 8: Schematic changes in the Southern Ocean during southern hemisphere warming intervals (Heinrich Stadial 1 and YD) and during cooling associated with the ACR (~14 ka). Sea ice expansion during the ACR suppressed air-sea gas exchange and deep-water CO_2 released and resulted in a northward shift of the Southern Hemisphere Westerlies (SHW) and upwelling of nutrient and Ba-rich waters. This shifted the centres of primary productivity towards the Subantarctic Zone, stimulating shallow-water coral growth, thick-walled benthic foraminiferal (*Uvigerina*) occurrence, and organic carbon accumulation. At the same time, increased stratification and reduced oxygen concentrations inhibited coral occurrence at depth and further south.

This article is protected by copyright. All rights reserved.

Accepted Article

7 References

Al-Horani, F. A., Al-Moghrabi, S. M., and de Beer, D., 2003, Microsensor study of photosynthesis and calcification in the scleractinian coral, Galaxea fascicularis: active internal carbon cycle: Journal of Experimental Marine Biology and Ecology, v. 288, no. 1, p. 1-15.

Anagnostou, E., Huang, K. F., You, C. F., Sikes, E. L., and Sherrell, R. M., 2012, Evaluation of boron isotope ratio as a pH proxy in the deep sea coral *Desmophyllum dianthus*: Evidence of physiological pH adjustment: Earth and Planetary Science Letters, v. 349–350, no. 0, p. 251-260.

Anagnostou, E., Sherrell, R. M., Gagnon, A., LaVigne, M., Field, M. P., and McDonough, W. F., 2011, Seawater nutrient and carbonate ion concentrations recorded as P/Ca, Ba/Ca, and U/Ca in the deep-sea coral Desmophyllum dianthus: Geochimica et Cosmochimica Acta, v. 75, no. 9, p. 2529-2543.

Anderson, R. F., Ali, S., Bradtmiller, L. I., Nielsen, S. H. H., Fleisher, M. Q., Anderson, B. E., and Burckle, L. H., 2009, Wind-Driven Upwelling in the Southern Ocean and the Deglacial Rise in Atmospheric CO_2: Science, v. 323, no. 5920, p. 1443-1448.

Anderson, R. F., Barker, S., Fleisher, M., Gersonde, R., Goldstein Steven, L., Kuhn, G., Mortyn, P. G., Pahnke, K., and Sachs Julian, P., 2014, Biological response to millennial variability of dust and nutrient supply in the Subantarctic South Atlantic Ocean: Philosophical Transactions of the Royal Society A: Mathematical, Physical and Engineering Sciences, v. 372, no. 2019, p. 20130054.

Anderson, R. F., Chase, Z., Fleisher, M. Q., and Sachs, J., 2002, The Southern Ocean's biological pump during the Last Glacial Maximum: Deep Sea Research Part II: Topical Studies in Oceanography, v. 49, no. 9, p. 1909-1938.

Barker, S., Diz, P., Vautravers, M. J., Pike, J., Knorr, G., Hall, I. R., and Broecker, W. S., 2009, Interhemispheric Atlantic seesaw response during the last deglaciation: Nature, v. 457, no. 7233, p. 1097-1102.

Bereiter, B., Eggleston, S., Schmitt, J., Nehrbass‐Ahles, C., Stocker Thomas, F., Fischer, H., Kipfstuhl, S., and Chappellaz, J., 2014, Revision of the EPICA Dome C CO_2 record from 800 to 600 kyr before present: Geophysical Research Letters, v. 42, no. 2, p. 542-549.

Bianchi, C., and Gersonde, R., 2004, Climate evolution at the last deglaciation: the role of the Southern Ocean: Earth and Planetary Science Letters, v. 228, no. 3, p. 407-424.

Blamart, D., Rollion-Bard, C., Meibom, A., Cuif, J. P., Juillet-Leclerc, A., and Dauphin, Y., 2007, Correlation of boron isotopic composition with ultrastructure in the deep-sea coral *Lophelia pertusa*: Implications for biomineralization and paleo-pH: Geochemistry, Geophysics, Geosystems, v. 8, no. 12, p. Q12001.

Blunier, T., Schwander, J., Stauffer, B., Stocker, T., Dällenbach, A., Indermühle, A., Tschumi, J., Chappellaz, J., Raynaud, D., and Barnola, J. M., 1997, Timing of the Antarctic cold reversal and the atmospheric CO_2 increase with respect to the Younger Dryas Event: Geophysical Research Letters, v. 24, no. 21, p. 2683-2686.

Boersma, A., 1986, Eocene/Oligocene Atlantic Paleo-Oceanography Using Benthic Foraminifera, *in* Pomerol, C., and Premoli-Silva, I., eds., Developments in Palaeontology and Stratigraphy, Volume 9, Elsevier, p. 225-236.

Boyle, E. A., 1981, Cadmium, zinc, copper, and barium in foraminifera tests: Earth and Planetary Science Letters, v. 53, no. 1, p. 11-35.

This article is protected by copyright. All rights reserved.

Accepted Article

Buizert, C., Adrian, B., Ahn, J., Albert, M., Alley, R. B., Baggenstos, D., Bauska, T. K., Bay, R. C., Bencivengo, B. B., Bentley, C. R., Brook, E. J., Chellman, N. J., Clow, G. D., Cole-Dai, J., Conway, H., Cravens, E., Cuffey, K. M., Dunbar, N. W., Edwards, J. S., Fegyveresi, J. M., Ferris, D. G., Fitzpatrick, J. J., Fudge, T. J., Gibson, C. J., Gkinis, V., Goetz, J. J., Gregory, S., Hargreaves, G. M., Iverson, N., Johnson, J. A., Jones, T. R., Kalk, M. L., Kippenhan, M. J., Koffman, B. G., Kreutz, K., Kuhl, T. W., Lebar, D. A., Lee, J. E., Marcott, S. A., Markle, B. R., Maselli, O. J., McConnell, J. R., McGwire, K. C., Mitchell, L. E., Mortensen, N. B., Neff, P. D., Nishiizumi, K., Nunn, R. M., J.Orsi, A., Pasteris, D. R., Pedro, J. B., Pettit, E. C., Price, P. B., Priscu, J. C., Rhodes, R. H., Rosen, J. L., Schauer, A. J., Schoenemann, S. W., Sendelbach, P. J., Severinghaus, J. P., Shturmakov, A. J., Sigl, M., Slawny, K. R., Souney, J. M., Sowers, T. A., Spencer, M. K., Steig, E. J., Taylor, K. C., Twickler, M. S., Vaughn, B. H., Voigt, D. E., Waddington, E. D., Welten, K. C., Wendricks, A. W., White, J. W. C., Winstrup, M., Wong, G. J., and Woodruff, T. E., 2015, Precise interpolar phasing of abrupt climate change during the last ice age: Nature, v. 520, p. 661-665.

Burke, A., and Robinson, L. F., 2012, The Southern Ocean's Role in Carbon Exchange During the Last Deglaciation: Science, v. 335, no. 6068, p. 557-561.

Burke, A., Robinson, L. F., McNichol, A. P., Jenkins, W. J., Scanlon, K. M., and Gerlach, D. S., 2010, Reconnaissance dating: A new radiocarbon method applied to assessing the temporal distribution of Southern Ocean deep-sea corals: Deep Sea Research Part I: Oceanographic Research Papers, v. 57, no. 11, p. 1510-1520.

Cardinal, D., Savoye, N., Trull, T. W., André, L., Kopczynska, E. E., and Dehairs, F., 2005, Variations of carbon remineralisation in the Southern Ocean illustrated by the Baxs proxy: Deep Sea Research Part I: Oceanographic Research Papers, v. 52, no. 2, p. 355-370.

Chan, L. H., Drummond, D., Edmond, J. M., and Grant, B., 1977, On the barium data from the Atlantic GEOSECS expedition: Deep Sea Research, v. 24, no. 7, p. 613-649.

Chen, T., Robinson, L. F., Beasley, M. P., Claxton, L. M., Andersen, M. B., Gregoire, L. J., Wadham, J., Fornari, D. J., and Harpp, K. S., 2016, Ocean mixing and ice-sheet control of seawater $^{234}U/^{238}U$ during the last deglaciation: Science, v. 354, no. 6312, p. 626-629.

Chen, T., Robinson, L. F., Burke, A., Southon, J., Spooner, P., Morris, P. J., and Ng, H. C., 2015, Synchronous centennial abrupt events in the ocean and atmosphere during the last deglaciation: Science, v. 349, no. 6255, p. 1537-1541.

Cheng, H., Adkins, J., Edwards, R. L., and Boyle, E. A., 2000, U-Th dating of deep-sea corals: Geochimica et Cosmochimica Acta, v. 64, no. 14, p. 2401-2416.

Crook, E. D., Cooper, H., Potts, D. C., Lambert, T., and Paytan, A., 2013, Impacts of food availability and pCO2 on planulation, juvenile survival, and calcification of the azooxanthellate scleractinian coral Balanophyllia elegans: Biogeosciences, v. 10, no. 11, p. 7599-7608.

Dodds, L. A., Roberts, J. M., Taylor, A. C., and Marubini, F., 2007, Metabolic tolerance of the cold-water coral *Lophelia pertusa* (Scleractinia) to temperature and dissolved oxygen change: Journal of Experimental Marine Biology and Ecology, v. 349, no. 2, p. 205-214.

Dumont, M., Pichevin, L., Geibert, W., Crosta, X., Michel, E., Moreton, S., Dobby, K., and Ganeshram, R., 2020, The nature of deep overturning and reconfigurations of the silicon cycle across the last deglaciation: Nature Communications, v. 11, no. 1, p. 1-11.

Ferrari, R., Jansen, M. F., Adkins, J. F., Burke, A., Stewart, A. L., and Thompson, A. F., 2014, Antarctic sea ice control on ocean circulation in present and glacial climates: Proceedings of the National Academy of Sciences, v. 111, no. 24, p. 8753-8758.

This article is protected by copyright. All rights reserved.

Accepted Article

Fogwill, C. J., Turney, C. S. M., Menviel, L., Baker, A., Weber, M. E., Ellis, B., Thomas, Z. A., Golledge, N. R., Etheridge, D., Rubino, M., Thornton, D. P., van Ommen, T. D., Moy, A. D., Curran, M. A. J., Davies, S., Bird, M. I., Munksgaard, N. C., Rootes, C. M., Millman, H., Vohra, J., Rivera, A., Mackintosh, A., Pike, J., Hall, I. R., Bagshaw, E. A., Rainsley, E., Bronk-Ramsey, C., Montenari, M., Cage, A. G., Harris, M. R. P., Jones, R., Power, A., Love, J., Young, J., Weyrich, L. S., and Cooper, A., 2020, Southern Ocean carbon sink enhanced by sea-ice feedbacks at the Antarctic Cold Reversal: Nature Geoscience, v. 13, p. 489–497.

Foster, G. L., 2008, Seawater pH, pCO_2 and [CO_3^{2-}] variations in the Caribbean Sea over the last 130 kyr: A boron isotope and B/Ca study of planktic foraminifera: Earth and Planetary Science Letters, v. 271, no. 1-4, p. 254-266.

Foster, G. L., Pogge von Strandmann, P. A. E., and Rae, J. W. B., 2010, Boron and magnesium isotopic composition of seawater: Geochemistry, Geophysics, Geosystems, v. 11, no. 8, p. Q08015.

Gagnon, A. C., Adkins, J. F., Fernandez, D. P., and Robinson, L. F., 2007, Sr/Ca and Mg/Ca vital effects correlated with skeletal architecture in a scleractinian deep-sea coral and the role of Rayleigh fractionation: Earth and Planetary Science Letters, v. 261, no. 1–2, p. 280-295.

Gagnon, A. C., Gothmann, A. M., Branson, O., Rae, J. W. B., and Stewart, J. A., 2021, Controls on boron isotopes in a cold-water coral and the cost of resilience to ocean acidification: Earth and Planetary Science Letters, v. 554, p. 116662.

Gooday, A. J., 1993, Deep-sea benthic foraminiferal species which exploit phytodetritus: Characteristic features and controls on distribution: Marine Micropaleontology, v. 22, no. 3, p. 187-205.

-, 2003, Benthic foraminifera (protista) as tools in deep-water palaeoceanography: Environmental influences on faunal characteristics, Advances in Marine Biology, Volume 46, Academic Press, p. 1-90.

Gooday, A. J., Levin, L. A., Linke, P., and Heeger, T., 1992, The Role of Benthic Foraminifera in Deep-Sea Food Webs and Carbon Cycling, *in* Rowe, G. T., and Pariente, V., eds., Deep-Sea Food Chains and the Global Carbon Cycle: Dordrecht, Springer Netherlands, p. 63-91.

Gori, A., Ferrier-Pagès, C., Hennige, S. J., Murray, F., Rottier, C., Wicks, L. C., and Roberts, J. M., 2016, Physiological response of the cold-water coral *Desmophyllum dianthus* to thermal stress and ocean acidification: PeerJ, v. 4, p. e1606.

Gottschalk, J., Skinner, L. C., Lippold, J., Vogel, H., Frank, N., Jaccard, S. L., and Waelbroeck, C., 2016, Biological and physical controls in the Southern Ocean on past millennial-scale atmospheric CO_2 changes: Nature Communications, v. 7, no. 1, p. 1-11.

Griffiths, J. S., Pan, T.-C. F., and Kelly, M. W., 2019, Differential responses to ocean acidification between populations of *Balanophyllia elegans* corals from high and low upwelling environments: Molecular Ecology, v. 28, no. 11, p. 2715-2730.

Guinotte, J. M., Orr, J., Cairns, S., Freiwald, A., Morgan, L., and George, R., 2006, Will human-induced changes in seawater chemistry alter the distribution of deep-sea scleractinian corals?: Frontiers in Ecology and the Environment, v. 4, no. 3, p. 141-146.

Gutjahr, M., Bordier, L., Douville, E., Farmer, J., Foster, G. L., Hathorne, E. C., Hönisch, B., Lemarchand, D., Louvat, P., McCulloch, M., Noireaux, J., Pallavicini, N., Rae, J. W. B., Rodushkin, I., Roux, P., Stewart, J. A., Thil, F., and You, C.-F., 2020, Sub-permil interlaboratory consistency for solution-based boron isotope analyses on marine carbonates Geostandards and Geoanalytical Research, v. 45, p. 59-75.

This article is protected by copyright. All rights reserved.

Accepted Article

Haddam, N. A., Michel, E., Siani, G., Licari, L., and Dewilde, F., 2020, Ventilation and Expansion of Intermediate and Deep Waters in the Southeast Pacific During the Last Termination: Paleoceanography and Paleoclimatology, v. 35, no. 7, p. e2019PA003743.

Harloff, J., and Mackensen, A., 1997, Recent benthic foraminiferal associations and ecology of the Scotia Sea and Argentine Basin: Marine Micropaleontology, v. 31, no. 1, p. 1-29.

Hines, S. K. V., Southon, J. R., and Adkins, J. F., 2015, A high-resolution record of Southern Ocean intermediate water radiocarbon over the past 30,000 years: Earth and Planetary Science Letters, v. 432, p. 46-58.

Hovland, M., 2008, Deep-water coral reefs: Unique biodiversity hot-spots, Springer Science & Business Media.

Jaccard, S. L., Galbraith, E. D., Martínez-García, A., and Anderson, R. F., 2016, Covariation of deep Southern Ocean oxygenation and atmospheric CO_2 through the last ice age: Nature, v. 530, p. 207-210

.

Kaiho, K., 1994, Benthic foraminiferal dissolved-oxygen index and dissolved-oxygen levels in the modern ocean: Geology, v. 22, no. 8, p. 719-722.

Kender, S., Aturamu, A., Zalasiewicz, J., Kaminski, M. A., and Williams, M., 2019, Benthic foraminifera indicate Glacial North Pacific Intermediate Water and reduced primary productivity over Bowers Ridge, Bering Sea, since the Mid-Brunhes Transition: J. Micropalaeontol., v. 38, no. 2, p. 177-187.

Klochko, K., Kaufman, A. J., Yao, W., Byrne, R. H., and Tossell, J. A., 2006, Experimental measurement of boron isotope fractionation in seawater: Earth and Planetary Science Letters, v. 248, no. 1–2, p. 276-285.

Li, T., Robinson, L. F., Chen, T., Wang, X. T., Burke, A., Rae, J. W. B., Pegrum-Haram, A., Knowles, T. D. J., Li, G., Chen, J., Ng, H. C., Prokopenko, M., Rowland, G., Samperiz, A., Stewart, J. A., Southon, J., and Spooner, P. T., 2020, Rapid shifts in circulation and biogeochemistry of the Southern Ocean during deglacial carbon cycle events: Science Advances, no. 42, p. eabb3807.

Lowry, D. P., Golledge, N. R., Menviel, L., and Bertler, N. A. N., 2019, Deglacial evolution of regional Antarctic climate and Southern Ocean conditions in transient climate simulations: Clim. Past, v. 15, no. 1, p. 189-215.

Marcott, S. A., Bauska, T. K., Buizert, C., Steig, E. J., Rosen, J. L., Cuffey, K. M., Fudge, T. J., Severinghaus, J. P., Ahn, J., Kalk, M. L., McConnell, J. R., Sowers, T., Taylor, K. C., White, J. W. C., and Brook, E. J., 2014, Centennial-scale changes in the global carbon cycle during the last deglaciation: Nature, v. 514, no. 7524, p. 616-619.

Margolin, A. R., Robinson, L. F., Burke, A., Waller, R. G., Scanlon, K. M., Roberts, M. L., Auro, M. E., and van de Flierdt, T., 2014, Temporal and spatial distributions of cold-water corals in the Drake Passage: Insights from the last 35,000 years: Deep Sea Research Part II: Topical Studies in Oceanography, v. 99, p. 237-248.

Markle, B. R., Steig, E. J., Roe, G. H., Winckler, G., and McConnell, J. R., 2018, Concomitant variability in high-latitude aerosols, water isotopes and the hydrologic cycle: Nature Geoscience, v. 11, no. 11, p. 853-859.

This article is protected by copyright. All rights reserved.

Accepted Article

Martin, P., Goodkin, N. F., Stewart, J. A., Foster, G. L., Sikes, E. L., White, H. K., Hennige, S., and Roberts, J. M., 2016, Deep-sea coral $\delta^{13}C$: A tool to reconstruct the difference between seawater pH and $\delta^{11}B$-derived calcifying fluid pH: Geophysical Research Letters, v. 43, no. 1, p. 299-308.

Martínez-Botí, M. A., Marino, G., Foster, G. L., Ziveri, P., Henehan, M. J., Rae, J. W. B., Mortyn, P. G., and Vance, D., 2015, Boron isotope evidence for oceanic carbon dioxide leakage during the last deglaciation: Nature, v. 518, no. 7538, p. 219-222.

Martínez-García, A., Sigman, D. M., Ren, H., Anderson, R. F., Straub, M., Hodell, D. A., Jaccard, S. L., Eglinton, T. I., and Haug, G. H., 2014, Iron Fertilization of the Subantarctic Ocean During the Last Ice Age: Science, v. 343, no. 6177, p. 1347-1350.

McCulloch, M., Trotter, J., Montagna, P., Falter, J., Dunbar, R., Freiwald, A., Försterra, G., López Correa, M., Maier, C., Rüggeberg, A., and Taviani, M., 2012, Resilience of cold-water scleractinian corals to ocean acidification: Boron isotopic systematics of pH and saturation state up-regulation: Geochimica et Cosmochimica Acta, v. 87, no. 0, p. 21-34.

McCulloch, R. D., Bentley, M. J., Purves, R. S., Hulton, N. R. J., Sugden, D. E., and Clapperton, C. M., 2000, Climatic inferences from glacial and palaeoecological evidence at the last glacial termination, southern South America: Journal of Quaternary Science, v. 15, no. 4, p. 409-417.

Menviel, L., Spence, P., Yu, J., Chamberlain, M. A., Matear, R. J., Meissner, K. J., and England, M. H., 2018, Southern Hemisphere westerlies as a driver of the early deglacial atmospheric CO2 rise: Nature Communications, v. 9, no. 1, p. 2503.

Montaggioni, L. F., Le Cornec, F., Corrège, T., and Cabioch, G., 2006, Coral barium/calcium record of mid-Holocene upwelling activity in New Caledonia, South-West Pacific: Palaeogeography, Palaeoclimatology, Palaeoecology, v. 237, no. 2, p. 436-455.

Olsen, A., Key, R. M., van Heuven, S., Lauvset, S. K., Velo, A., Lin, X., Schirnick, C., Kozyr, A., Tanhua, T., Hoppema, M., Jutterström, S., Steinfeldt, R., Jeansson, E., Ishii, M., Pérez, F. F., and Suzuki, T., 2016, The Global Ocean Data Analysis Project version 2 (GLODAPv2) – an internally consistent data product for the world ocean: Earth Syst. Sci. Data, v. 8, no. 2, p. 297-323.

Parrenin, F., Masson-Delmotte, V., Köhler, P., Raynaud, D., Paillard, D., Schwander, J., Barbante, C., Landais, A., Wegner, A., and Jouzel, J., 2013, Synchronous Change of Atmospheric CO_2 and Antarctic Temperature During the Last Deglacial Warming: Science, v. 339, no. 6123, p. 1060-1063.

Peck, V. L., Allen, C. S., Kender, S., McClymont, E. L., and Hodgson, D. A., 2015, Oceanographic variability on the West Antarctic Peninsula during the Holocene and the influence of upper circumpolar deep water: Quaternary Science Reviews, v. 119, p. 54-65.

Pedro, J. B., Bostock, H. C., Bitz, C. M., He, F., Vandergoes, M. J., Steig, E. J., Chase, B. M., Krause, C. E., Rasmussen, S. O., Markle, B. R., and Cortese, G., 2016, The spatial extent and dynamics of the Antarctic Cold Reversal: Nature Geoscience, v. 9, no. 1, p. 51-55.

Piña-Ochoa, E., Høgslund, S., Geslin, E., Cedhagen, T., Revsbech, N. P., Nielsen, L. P., Schweizer, M., Jorissen, F., Rysgaard, S., and Risgaard-Petersen, N., 2010, Widespread occurrence of nitrate storage and denitrification among Foraminifera and *Gromiida*: Proceedings of the National Academy of Sciences, v. 107, no. 3, p. 1148-1153.

Purser, A., Orejas, C., Moje, A., and Thomsen, L., 2014, The influence of flow velocity and suspended particulate concentration on net prey capture rates by the scleractinian coral *Balanophyllia europaea* (Scleractinia: Dendrophylliidae): Journal of the Marine Biological Association of the United Kingdom, v. 94, no. 4, p. 687-696.

This article is protected by copyright. All rights reserved.

Accepted Article

Putnam, A. E., Denton, G. H., Schaefer, J. M., Barrell, D. J. A., Andersen, B. G., Finkel, R. C., Schwartz, R., Doughty, A. M., Kaplan, M. R., and Schlüchter, C., 2010, Glacier advance in southern middle-latitudes during the Antarctic Cold Reversal: Nature Geoscience, v. 3, no. 10, p. 700-704.

Rae, J. W. B., 2018, Boron Isotopes in Foraminifera: Systematics, Biomineralisation, and CO2 Reconstruction, *in* Marschall, H., and Foster, G., eds., Boron Isotopes: The Fifth Element: Cham, Springer International Publishing, p. 107-143.

Rae, J. W. B., Burke, A., Robinson, L. F., Adkins, J. F., Chen, T., Cole, C., Greenop, R., Li, T., Littley, E. F. M., Nita, D. C., Stewart, J. A., and Taylor, B. J., 2018, CO_2 storage and release in the deep Southern Ocean on millennial to centennial timescales: Nature, v. 562, no. 7728, p. 569-573.

Rae, J. W. B., Foster, G. L., Schmidt, D. N., and Elliott, T., 2011, Boron isotopes and B/Ca in benthic foraminifera: Proxies for the deep ocean carbonate system: Earth and Planetary Science Letters, v. 302, no. 3-4, p. 403-413.

Roberts, J., Gottschalk, J., Skinner, L. C., Peck, V. L., Kender, S., Elderfield, H., Waelbroeck, C., Vázquez Riveiros, N., and Hodell, D. A., 2016, Evolution of South Atlantic density and chemical stratification across the last deglaciation: Proceedings of the National Academy of Sciences, v. 113, no. 3, p. 514-519.

Roberts, J., McCave, I. N., McClymont, E. L., Kender, S., Hillenbrand, C. D., Matano, R., Hodell, D. A., and Peck, V. L., 2017, Deglacial changes in flow and frontal structure through the Drake Passage: Earth and Planetary Science Letters, v. 474, p. 397-408.

Roberts, J. M., Wheeler, A. J., and Freiwald, A., 2006, Reefs of the Deep: The Biology and Geology of Cold-Water Coral Ecosystems: Science, v. 312, no. 5773, p. 543-547.

Schumacher, S., Jorissen, F. J., Dissard, D., Larkin, K. E., and Gooday, A. J., 2007, Live (Rose Bengal stained) and dead benthic foraminifera from the oxygen minimum zone of the Pakistan continental margin (Arabian Sea): Marine Micropaleontology, v. 62, no. 1, p. 45-73.

Spooner, P. T., Chen, T., Robinson, L. F., and Coath, C. D., 2016, Rapid uranium-series age screening of carbonates by laser ablation mass spectrometry: Quaternary Geochronology, v. 31, p. 28-39.

Spooner, P. T., Robinson, L. F., Hemsing, F., Morris, P., and Stewart, J. A., 2018, Extended calibration of cold-water coral Ba/Ca using multiple genera and co-located measurements of dissolved barium concentration: Chemical Geology, v. 499, p. 100-110.

Stephens, B. B., and Keeling, R. F., 2000, The influence of Antarctic sea ice on glacial–interglacial CO_2 variations: Nature, v. 404, no. 6774, p. 171-174.

Stewart, J. A., Anagnostou, E., and Foster, G. L., 2016, An improved boron isotope pH proxy calibration for the deep-sea coral *Desmophyllum dianthus* through sub-sampling of fibrous aragonite: Chemical Geology, v. 447, p. 148-160.

Stewart, J. A., Christopher, S. J., Kucklick, J. R., Bordier, L., Chalk, T. B., Dapoigny, A., Douville, E., Foster, G. L., Gray, W. R., Greenop, R., Gutjahr, M., Hemsing, F., Henehan, M. J., Holdship, P., Hsieh, Y.-T., Kolevica, A., Lin, Y.-P., Mawbey, E. M., Rae, J. W. B., Robinson, L. F., Shuttleworth, R., You, C.-F., Zhang, S., and Day, R. D., 2020, NIST RM 8301 Boron Isotopes in Marine Carbonate (Simulated Coral and Foraminifera Solutions): Inter-laboratory δ11B and trace element ratio value assignment: Geostandards and Geoanalytical Research, v. 45, p. 77-96.

Stroobants, N., Dehairs, F., Goeyens, L., Vanderheijden, N., and Van Grieken, R., 1991, Barite formation in the Southern Ocean water column: Marine Chemistry, v. 35, no. 1, p. 411-421.

This article is protected by copyright. All rights reserved.

Thiagarajan, N., Gerlach, D., Roberts Mark, L., Burke, A., McNichol, A., Jenkins William, J., Subhas Adam, V., Thresher Ronald, E., and Adkins Jess, F., 2013, Movement of deep‐sea coral populations on climatic timescales: Paleoceanography, v. 28, no. 2, p. 227-236.

Toggweiler, J. R., 2009, Shifting westerlies: Science, v. 323, no. 5920, p. 1434-1435.

Wang, X. T., Sigman, D. M., Prokopenko, M. G., Adkins, J. F., Robinson, L. F., Hines, S. K., Chai, J., Studer, A. S., Martínez-García, A., Chen, T., and Haug, G. H., 2017, Deep-sea coral evidence for lower Southern Ocean surface nitrate concentrations during the last ice age: Proceedings of the National Academy of Sciences, v. 114, no. 13, p. 3352-3357.

Watson, A. J., and Naveira Garabato, A. C., 2006, The role of Southern Ocean mixing and upwelling in glacial-interglacial atmospheric CO_2 change: Tellus B: Chemical and Physical Meteorology, v. 58, no. 1, p. 73-87.

Zeebe, R. E., and Rae, J. W. B., 2020, Equilibria, kinetics, and boron isotope partitioning in the aqueous boric acid–hydrofluoric acid system: Chemical Geology, v. 550, p. 119693.

Zeebe, R. E., and Wolf-Gladrow, D. A., 2001, CO_2 in seawater: equilibrium, kinetics, isotopes, Amsterdam, The Netherlands, Elsevier, Elsevier Oceanography Series.

Accepted Article

This article is protected by copyright. All rights reserved.

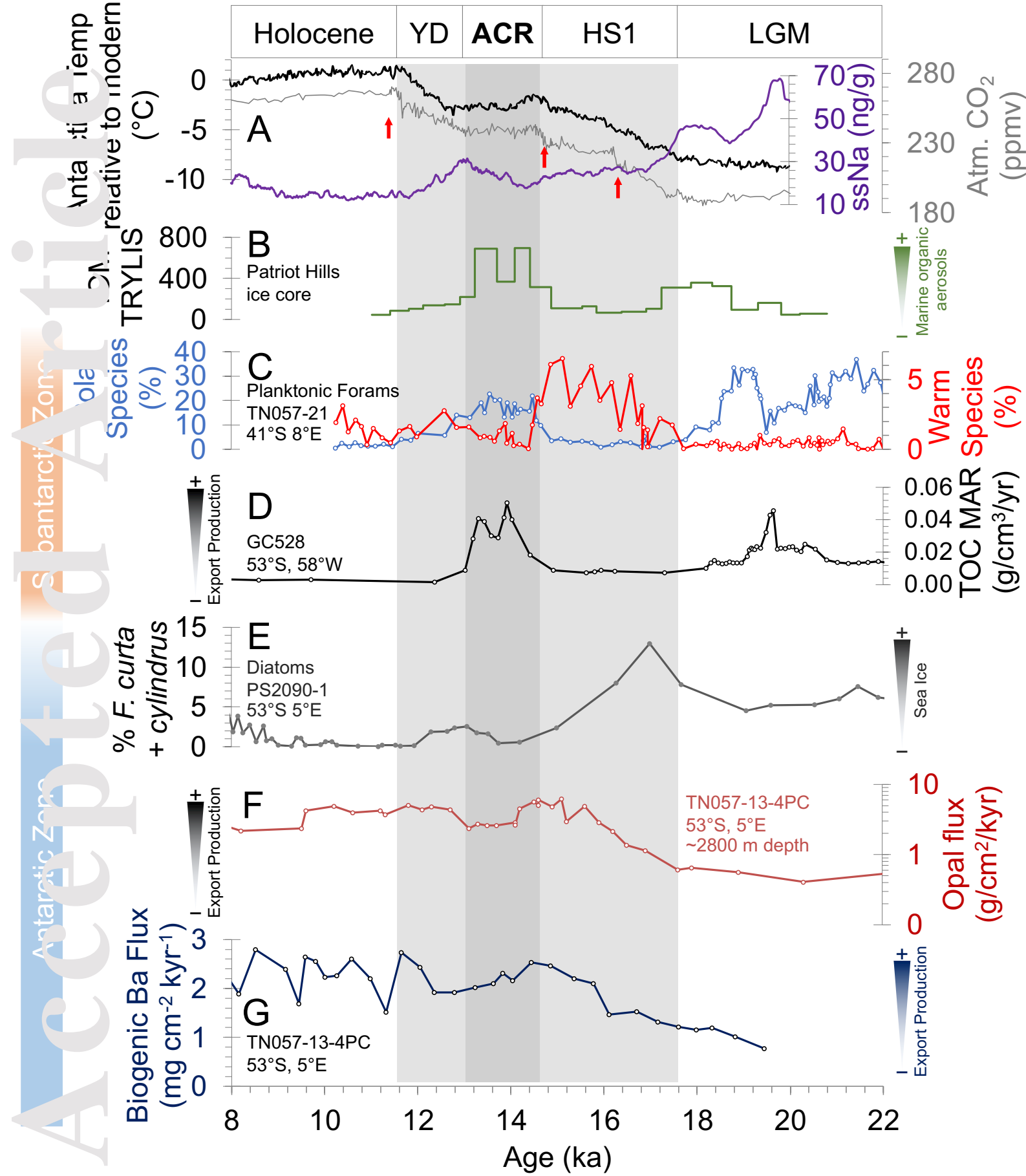

Accepted Article

This article has been accepted for publication and undergone full peer review but has not been through the copyediting, typesetting, pagination and proofreading process, which may lead to differences between this version and the Version of Record. Please cite this article as doi: 10.1029/2021PA004288.

This article is protected by copyright. All rights reserved.

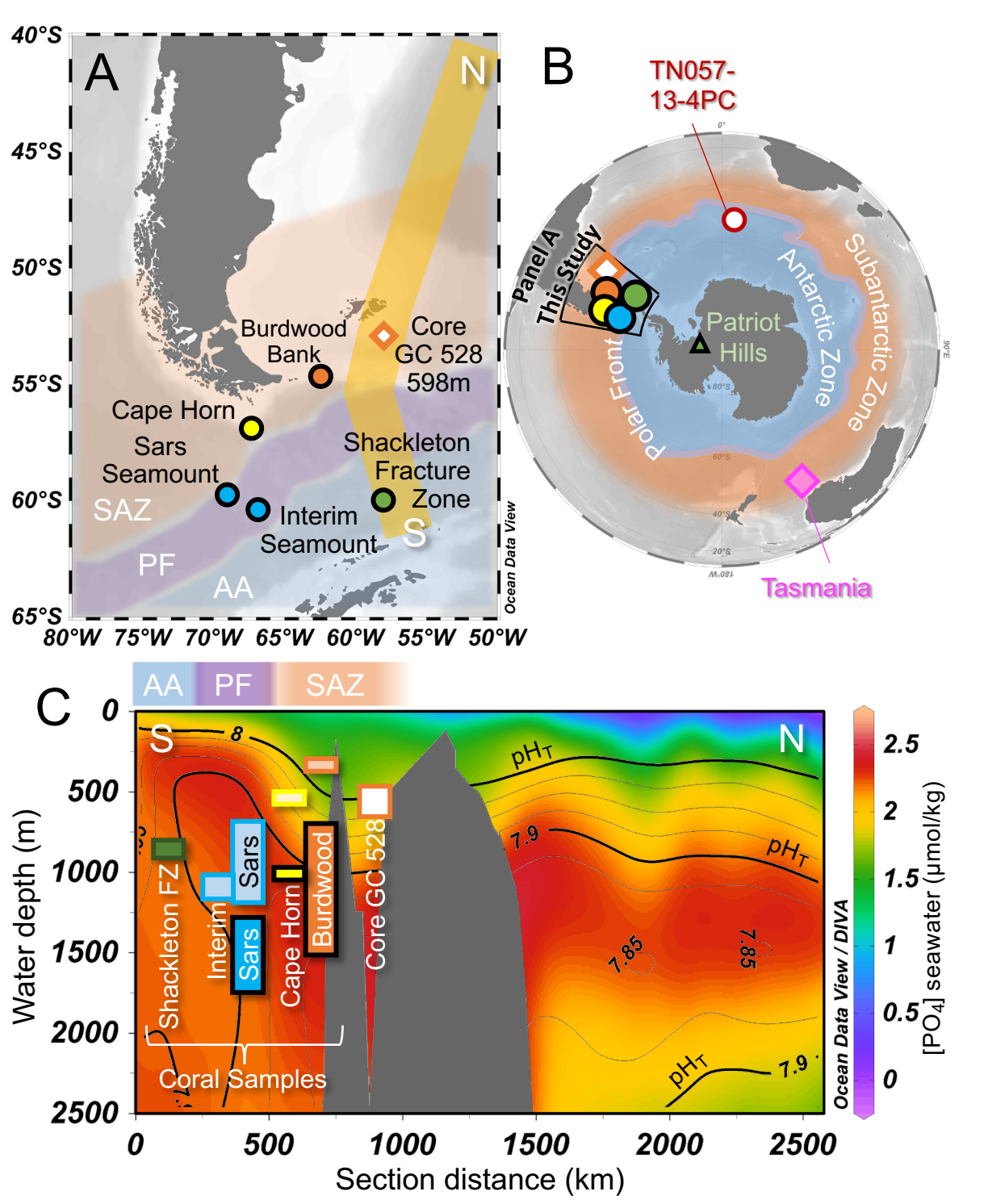
A
N
S
Burdwood Bank
Core GC 528 598m
Cape Horn
Sars Seamount
Shackleton Fracture Zone
Interim Seamount
SAZ
PF
AA
40°S
45°S
50°S
55°S
60°S
65°S
80°W 75°W 70°W 65°W 60°W 55°W 50°W
Ocean Data View
B
TN057-13-4PC
Panel A This Study
Patriot Hills
Antarctic Zone
Subantarctic Zone
Polar Front
Tasmania
C
AA
PF
SAZ
S
N
8
7.9
7.85
pHT
Shackleton FZ
Interim Sars
Sars
Cape Horn
Burdwood
Core GC 528
Coral Samples
Water depth (m)
0
500
1000
1500
2000
2500
Section distance (km)
Ocean Data View / DIVA
[PO4] seawater (µmol/kg)
2.5
2
1.5
1
0.5
0

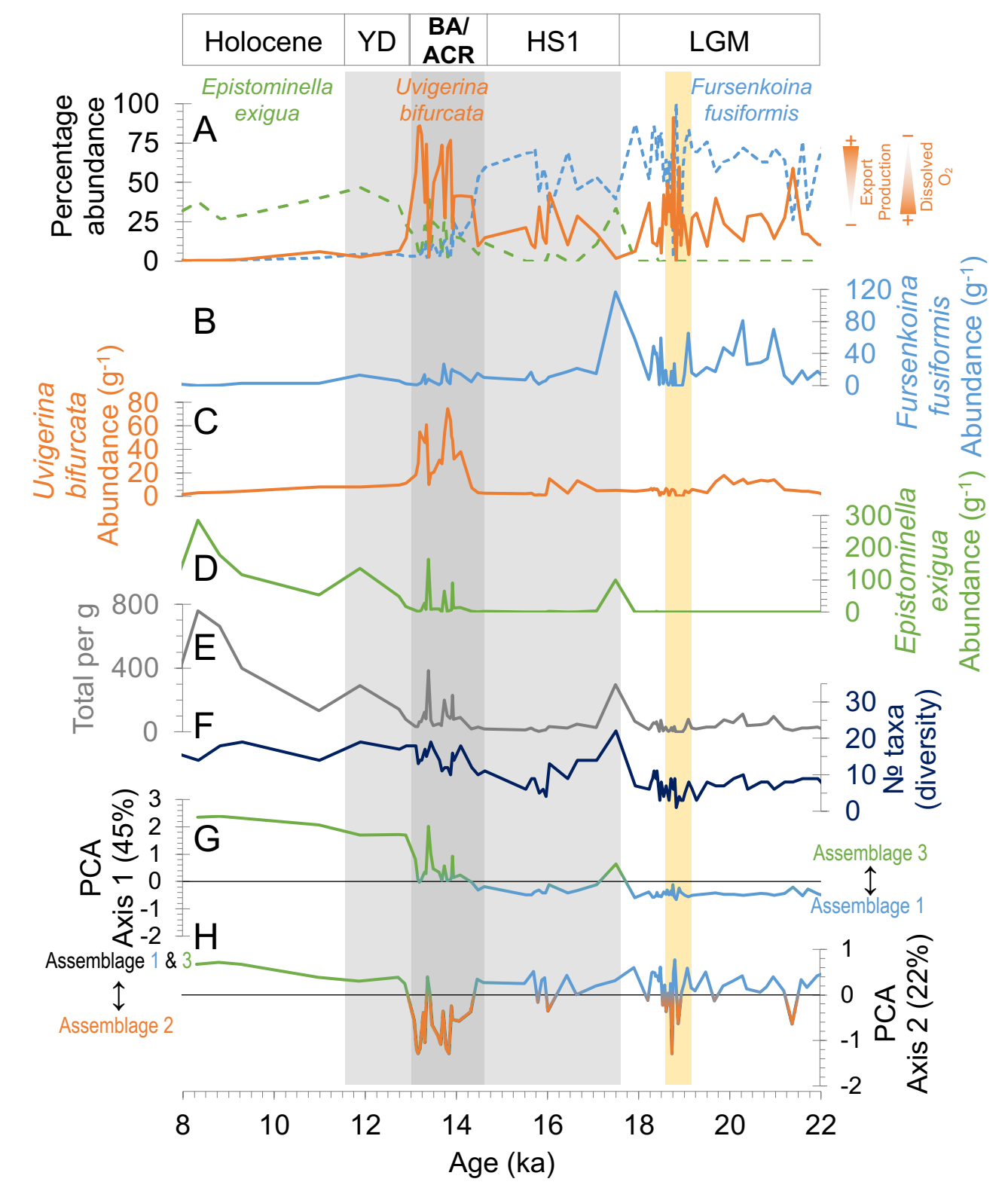
Holocene
YD
BA/ ACR
HS1
LGM
Epistominella exigua
Uvigerina bifurcata
Fursenkoina fusiformis
Percentage abundance
A
Export Production
Dissolved O2
B
C
D
E
F
G
H
Uvigerina bifurcata Abundance (g-1)
Fursenkoina fusiformis Abundance (g-1)
Epistominella exigua Abundance (g-1)
Total per g
№ taxa (diversity)
PCA Axis 1 (45%)
Assemblage 3
Assemblage 1
Assemblage 1 & 3
Assemblage 2
PCA Axis 2 (22%)
Age (ka)

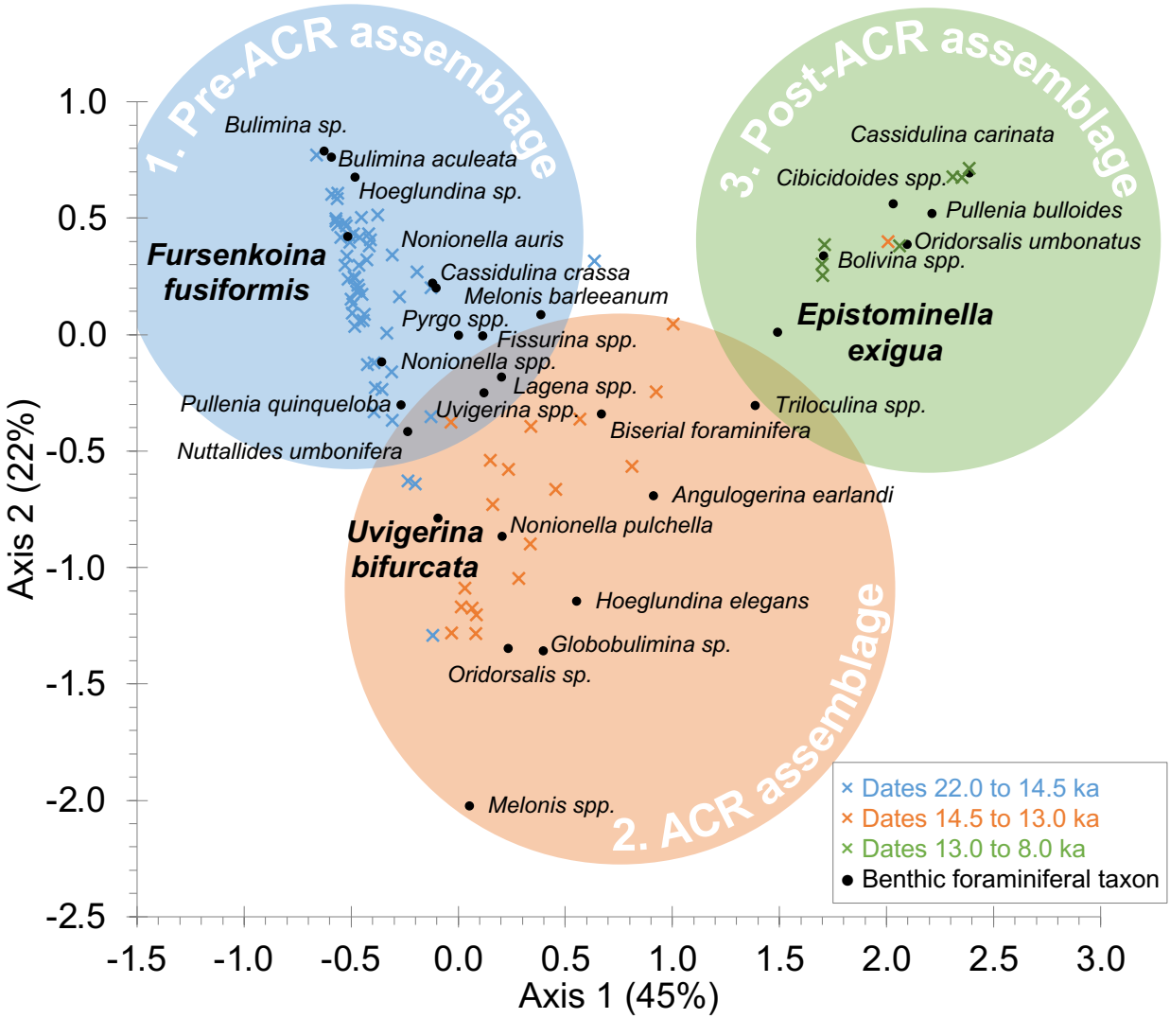
1. Pre-ACR assemblage
2. ACR assemblage
3. Post-ACR assemblage
Bulimina sp.
Bulimina aculeata
Hoeglundina sp.
Fursenkoina fusiformis
Nonionella auris
Cassidulina crassa
Melonis barleeanum
Pyrgo spp.
Fissurina spp.
Nonionella spp.
Lagena spp.
Pullenia quinqueloba
Uvigerina spp.
Nuttallides umbonifera
Biserial foraminifera
Triloculina spp.
Angulogerina earlandi
Uvigerina bifurcata
Nonionella pulchella
Hoeglundina elegans
Globobulimina sp.
Oridorsalis sp.
Melonis spp.
Cassidulina carinata
Cibicidoides spp.
Pullenia bulloides
Oridorsalis umbonatus
Bolivina spp.
Epistominella exigua
Dates 22.0 to 14.5 ka
Dates 14.5 to 13.0 ka
Dates 13.0 to 8.0 ka
Benthic foraminiferal taxon
Axis 2 (22%)
Axis 1 (45%)
1.0
0.5
0.0
-0.5
-1.0
-1.5
-2.0
-2.5
-1.5
-1.0
-0.5
0.0
0.5
1.0
1.5
2.0
2.5
3.0

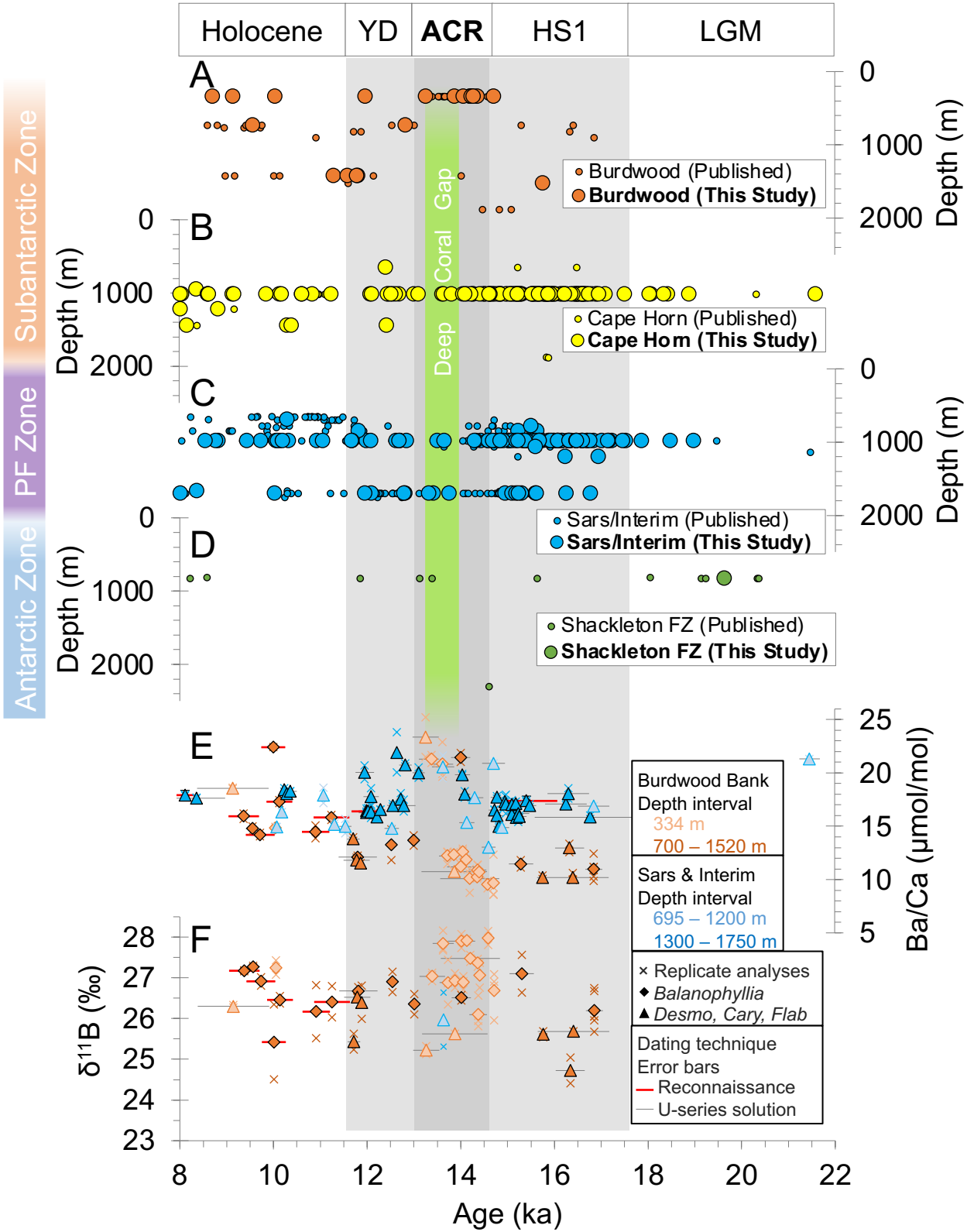
Holocene
YD
ACR
HS1
LGM
Subantarctic Zone
PF Zone
Antarctic Zone
Coral Gap
Deep
A
B
C
D
E
F
Burdwood (Published)
Burdwood (This Study)
Cape Horn (Published)
Cape Horn (This Study)
Sars/Interim (Published)
Sars/Interim (This Study)
Shackleton FZ (Published)
Shackleton FZ (This Study)
Depth (m)
0
1000
2000
Burdwood Bank
Depth interval
334 m
700 – 1520 m
Sars & Interim
Depth interval
695 – 1200 m
1300 – 1750 m
Ba/Ca (µmol/mol)
5
10
15
20
25
× Replicate analyses
◆ Balanophyllia
▲ Desmo, Cary, Flab
Dating technique
Error bars
Reconnaissance
U-series solution
δ11B (‰)
23
24
25
26
27
28
8
10
12
14
16
18
20
22
Age (ka)

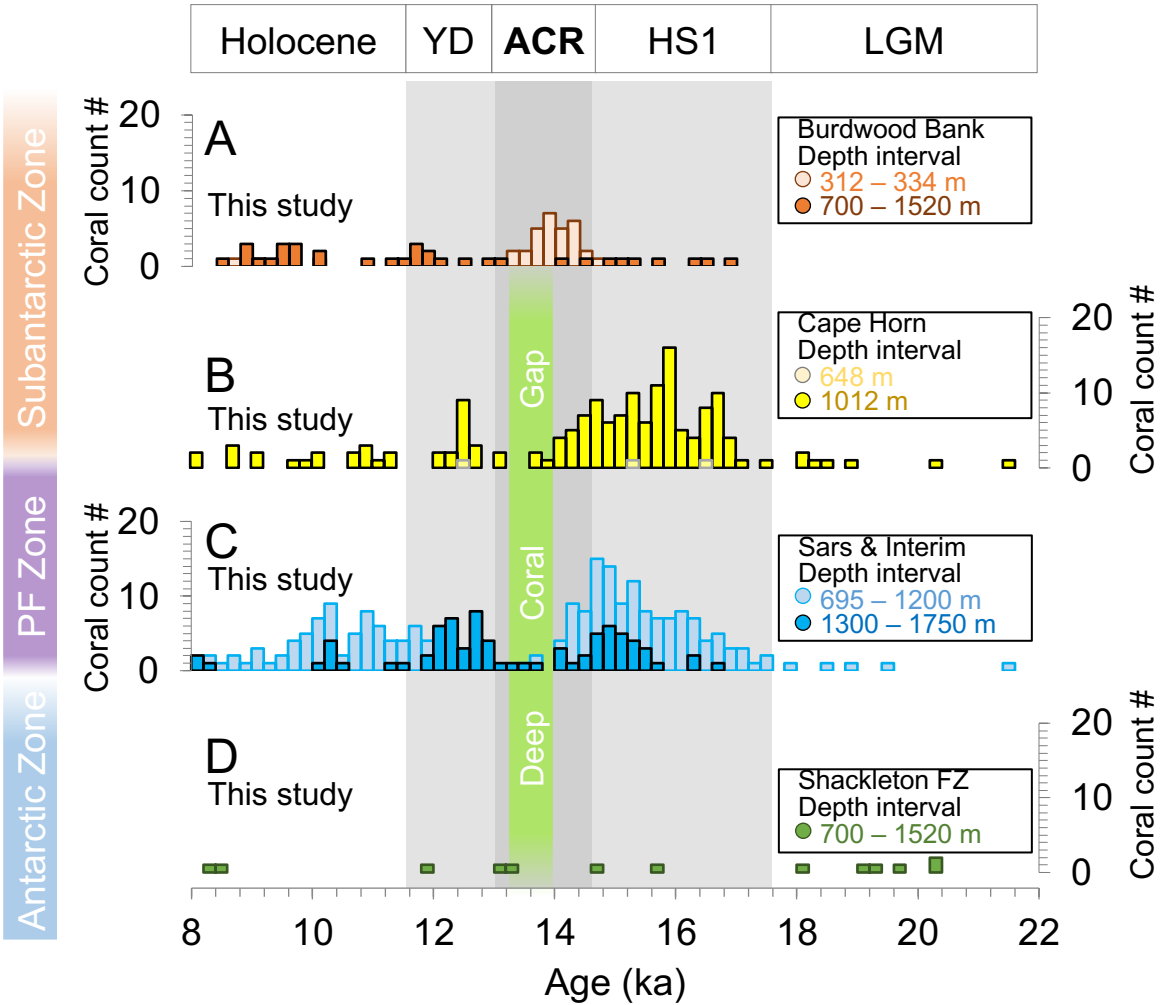
Holocene
YD
ACR
HS1
LGM
Subantarctic Zone
PF Zone
Antarctic Zone
A
This study
Coral count #
20
10
0
Burdwood Bank
Depth interval
312 – 334 m
700 – 1520 m
B
This study
Gap
Cape Horn
Depth interval
648 m
1012 m
C
This study
Coral
Sars & Interim
Depth interval
695 – 1200 m
1300 – 1750 m
D
This study
Deep
Shackleton FZ
Depth interval
700 – 1520 m
8
10
12
14
16
18
20
22
Age (ka)

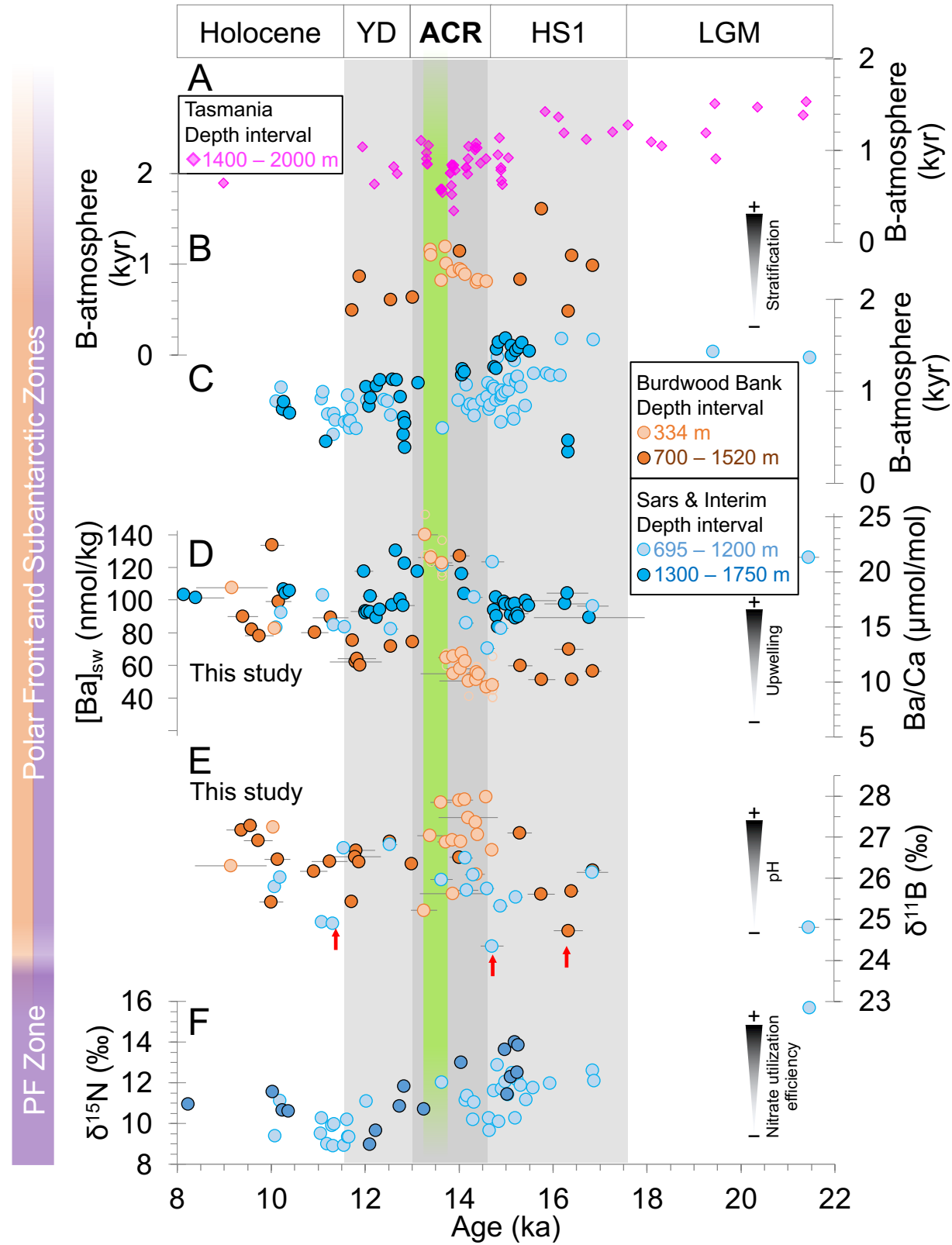
Holocene
YD
ACR
HS1
LGM
A
Tasmania
Depth interval
1400 – 2000 m
B
B-atmosphere (kyr)
C
Burdwood Bank
Depth interval
334 m
700 – 1520 m
Sars & Interim
Depth interval
695 – 1200 m
1300 – 1750 m
Stratification
D
[Ba]sw (nmol/kg)
This study
Upwelling
Ba/Ca (µmol/mol)
E
This study
pH
δ11B (‰)
F
δ15N (‰)
Nitrate utilization efficiency
Age (ka)
Polar Front and Subantarctic Zones
PF Zone

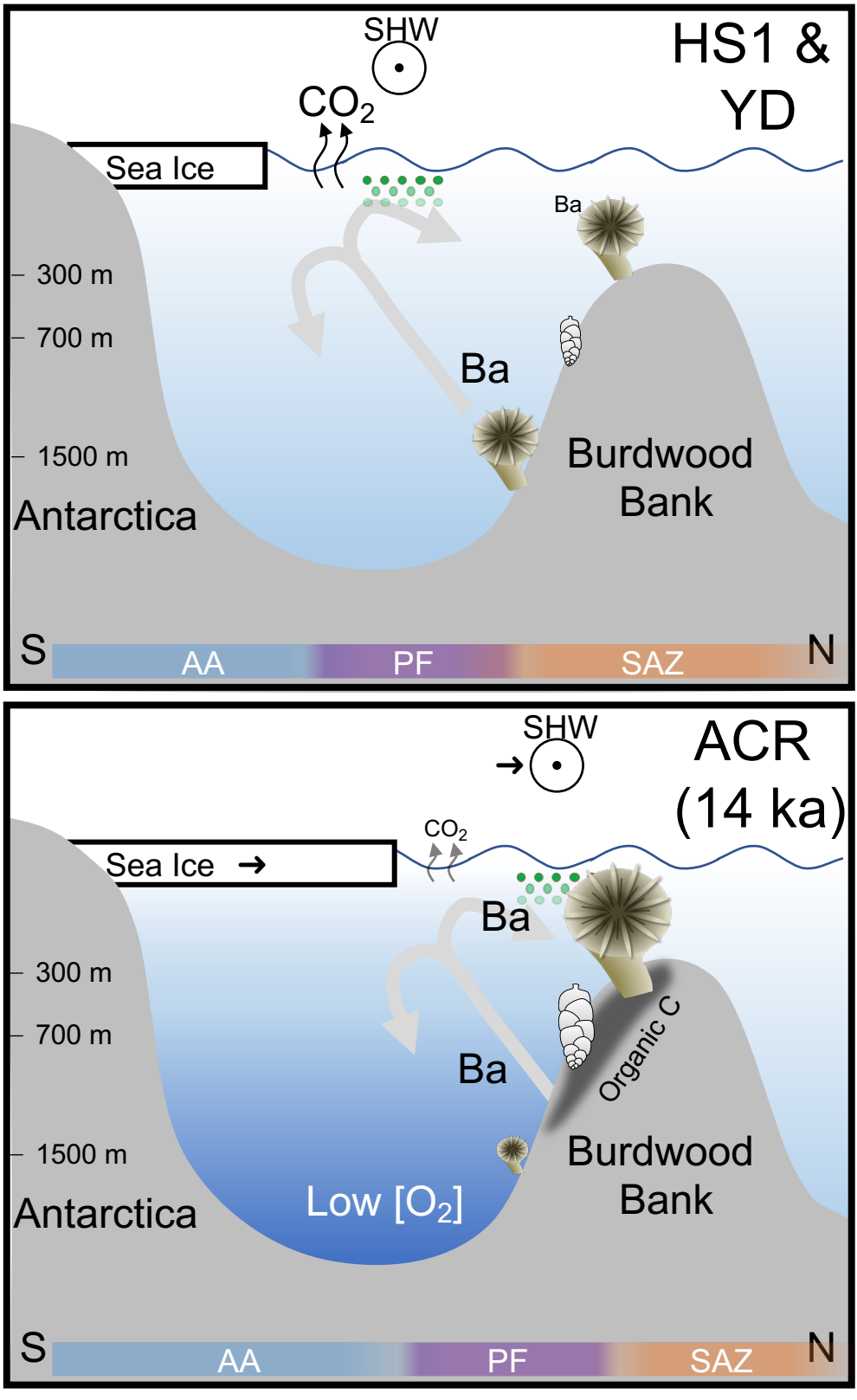
HS1 &
YD
SHW
CO_2
Sea Ice
Ba
300 m
700 m
1500 m
Ba
Burdwood
Bank
Antarctica
S
AA
PF
SAZ
N
ACR
(14 ka)
SHW
CO_2
Sea Ice
Ba
300 m
700 m
Ba
Organic C
1500 m
Burdwood
Bank
Low [O_2]
Antarctica
S
AA
PF
SAZ
N